https://doi.org/10.1016/j.engappai.2021.104314

QANA: Quantum-based avian navigator algorithm for global optimization and its engineering applications

Hoda Zamani[1, 2], Mohammad H. Nadimi-Shahraki[1, 2*], Amir H. Gandomi[3]

[1]Faculty of Computer Engineering, Najafabad Branch, Islamic Azad University, Najafabad, Iran
[2]Big Data Research Center, Najafabad Branch, Islamic Azad University, Najafabad, Iran
[3]Faculty of Engineering & Information Technology, University of Technology Sydney, Australia
[*]Corresponding: nadimi@iaun.ac.ir & nadimi@ieee.org, Offi.tel: +98-3142292632.

Abstract. Differential evolution (DE) is an efficient approach widely applied for solving global optimization problems. Nevertheless, it suffers from some drawbacks, such as weak local searchability, premature convergence, and low effectiveness and scalability when the dimension is increased. This paper proposes a novel DE algorithm named quantum-based avian navigator algorithm (QANA), which mimics migratory birds' extraordinary precision navigation during long-distance aerial paths. The QANA is modeled by introducing two long-term and short-term memories, a new V-echelon communication topology, and quantum-based navigation, including two mutation strategies and a qubit-crossover operator. Moreover, a success-based population distribution (SPD) policy is proposed to assign the flocks' mutation strategies using the previous success rate of the strategies. The effectiveness and scalability of the proposed QANA were experimentally determined using benchmark functions CEC 2018 and CEC 2013 as LSGO problems, and the results were statistically analyzed by the Wilcoxon signed-rank sum test, ANOVA, and mean absolute error. Finally, the applicability of the QANA to solve real-world problems was evaluated by four engineering problems. The experimental results and statistical analysis prove that the QANA is superior to the competitor DE and swarm intelligence algorithms.

Keywords: Optimization, Metaheuristic algorithms, Differential evolution algorithms, Large-scale global optimization, Quantum computing, Engineering optimization problems.

1. Introduction

Solving global optimization problems in real-world applications in the medical, engineering (He et al., 2020; Wu et al., 2019), industrial (Dezfouli et al., 2018; Sayarshad, 2010; Zahrani et al., 2021), and other fields face various complexities, including non-linearly, non-convex, multi-modality, non-differentiable functions, and large-scale dimensionality (Deb and Myburgh, 2017; Gandomi et al., 2019). Since these challenges and the available search time do not allow the use of exact optimization algorithms, many metaheuristic algorithms have been developed, which can seek reasonable solutions to solve these complex problems.

The metaheuristic algorithms are inspired mainly by the collective behaviors of swarms and evolutionary phenomena in nature (Eiben and Smith, 2015; Talbi, 2009) and can be classified into three main categories: swarm intelligence (SI), physics, and evolutionary algorithms (EAs) (Talbi, 2009; Zamani et al., 2019).

The SI algorithms are inspired by the behaviors of swarms of birds (Yang and Gandomi, 2012), aquatic animals (Gandomi and Alavi, 2012; Mirjalili and Lewis, 2016), terrestrial animals (Long et al., 2018; Mirjalili et al., 2014), and insects (Karaboga and Basturk, 2007) in nature. They have been rapidly extended, and their performance and abilities make them suitable for solving a wide range of complex problems (Abdel-Basset et al., 2020; Altabeeb et al., 2019; Zamani and Nadimi-Shahraki, 2016). Meanwhile, they are also adapted mostly by using transfer functions (Taghian et al., 2018) to introduce effective algorithms (Mafarja et al., 2019; Pashaei and Aydin, 2017; Srikanth et al., 2018; Taghian and Nadimi-Shahraki, 2019a, b; Vieira et al., 2013; Zhang et al., 2016) to solve a wide variety of discrete optimization problems (Karasu et al., 2020). Recently, numerous SI algorithms have been proposed by introducing new approaches (Abdel-Basset et al., 2020; Banaie-Dezfouli et al., 2021; Long et al., 2018; Nadimi-Shahraki et al., 2020a; Sun et al., 2018) to solve their weaknesses.

Physics-based algorithms are suggested based on the physical concepts in nature to solve numerical optimization problems. These algorithms generate the new candidate solutions using physical laws, such as gravitational force, magnetic, chemical reaction, light refraction, inertia force, and molecular dynamics to eventually guide the search process to the promising area by increasing the exploitation ability. The most recent algorithms in this category are simulated annealing (SA) (Kirkpatrick et al., 1983), ray optimization (RO) (Kaveh and Khayatazad, 2012), black hole (BH) (Hatamlou, 2013), magnetic optimization algorithms (MOAs) (Tayarani-N and Akbarzadeh-T, 2014), and quantum-inspired gravitational search algorithm (QIGSA) (Soleimanpour-Moghadam et al., 2014).

In evolutionary algorithms (EAs), the problems are approximated by performing meaningful search strategies inspired by biological evolution, such as reproduction, mutation, recombination, and selection (Eiben and Smith, 2015; Price et al., 2006; Qin et al., 2008; Wu et al., 2016; Zhang and Sanderson, 2009). The EAs initiate random candidate solutions and iteratively generate and evolve offspring solutions until the acceptable solution is discovered. The prominent representatives of EAs include evolution strategies (ES) (Beyer and Schwefel, 2002), estimation of distribution algorithms (EDAs) (Larrañaga and Lozano, 2001), biogeography-based optimization (BBO) (Simon, 2008), opposition-based DE (ODE) (Rahnamayan et al., 2008), and differential evolution (DE) (Storn and Price, 1995, 1997).

Since the introduction of the DE algorithm by Storn and Price (Storn and Price, 1995, 1997), it has become one of the most successful evolutionary algorithms in dealing with complex optimization problems (Brest et al., 2006; Brest et al., 2016; Islam et al., 2011;

Mallipeddi and Suganthan, 2010; Maučec and Brest, 2019). The DE algorithms incorporate mutation, crossover, and selection operators to gradually move the population toward the global optimum during the optimization process (Wu et al., 2016; Yang et al., 2008). However, the original DE algorithms suffer from premature convergence and population stagnation, which can significantly affect its performance. Therefore, many DE developments have been proposed to cope with their weaknesses by introducing novel approaches and successful enhancements (Cai and Wang, 2015; Civicioglu et al., 2020; Deng et al., 2017; Mallipeddi and Suganthan, 2010; Mallipeddi et al., 2011; Meng and Pan, 2016; Nadimi-Shahraki et al., 2020b; Wang et al., 2013; Wang et al., 2011; Wang et al., 2014). Therefore, as shown in Fig. (1), the DE algorithm's development can be classified based on these introduced approaches and mechanisms as follows.

Trial vector generation strategies: The performance of the DE is sensitive to the search strategies (Awad et al., 2016b; Meng and Pan, 2018; Qin et al., 2008; Wang et al., 2011; Zhang and Sanderson, 2009), and an inappropriate choice can generate unpromising trial vectors that may lead to premature convergence, local optima trapping, and low diversity and scalability (Brest et al., 2016, 2017; Fan and Lampinen, 2003; Larrañaga and Lozano, 2001; Tanabe and Fukunaga, 2013; Wu et al., 2018; Yang et al., 2008). Therefore, to improve the DE algorithm, there has been a growing trend to enhance the trial vector generation strategies, which has been introduced by a variety of mutations and crossover operators.

The most common mutation strategies are DE/rand/1 (Storn and Price, 1997), DE/rand/2 (Qin et al., 2008), DE/best/1, and DE/best/2. The mutation strategies DE/best/1 and DE/best/2 effectively solve unimodal problems; however, they usually demonstrate a slow convergence rate when dealing with multimodal problems because of their greediness. As such, improved standard mutation strategies have been introduced using L-SHADE (Tanabe and Fukunaga, 2014), iLSHADE (Brest et al., 2016), jSO (Brest et al., 2017), and PALM-DE (Meng et al., 2018) to straightforwardly adjust the balance between diversify and convergence rate. The DE/current-to-pbest (Zhang and Sanderson, 2009), DE/current-to-gr_best/1 (Ghosh et al., 2011), ensemble mutation by using three strategies (DE/rand/1, DE/current-to-rand/1 and DE/best/2) (Mallipeddi and Suganthan, 2010), improved DE/rand/2 strategy (Wang et al., 2018), and trigonometric (Fan and Lampinen, 2003) are some advanced mutation strategies that enhance the performance of DE for solving complex problems. Gong et al. (Gong et al., 2010) proposed the DE/BBO algorithm by incorporating DE's mutation operator by utilizing the migration operator in the BBO algorithm (Simon, 2008).

The crossover operator aims to intensify the population diversity (Awad et al., 2016b; Maučec and Brest, 2019; Wang et al., 2012) by exchanging elements between the mutant and parent vectors. In recent years, various crossover strategies have been introduced, including JADE (Zhang and Sanderson, 2009), CPI-DE [27], CoBiDE (Wang et al., 2014), DE-EIG [29], HLXDE (Cai and Wang, 2015), multiple exponential recombinations [32], and MDE_pBX (Islam et al., 2011). Moreover, Deng et al. (Deng et al., 2017) developed a new rotating crossover scheme (DE-RCO) to enlarge the diversity of the population and enhance the searching ability by utilizing a multi-angle searching strategy-based rotating crossover operator (RCO). Wang et al. (Wang et al., 2012) proposed the orthogonal crossover (OX) operator based on orthogonal design, which creates a systematic and rational search in the region defined by the parent solutions. Recently, an adaptive guided differential evolution (AGDE) algorithm was proposed (Houssein et al., 2021), which introduces a new mutation rule and an adapted parameter value for effective crossover strategies.

Population: The effectiveness of DE algorithms critically depends on how each utilizes the population in terms of initializing, size-changing, and using multi-populations. Although the population is usually initialized randomly (Brest et al., 2016; Storn and Price, 1997; Tanabe and Fukunaga, 2013; Zhang and Sanderson, 2009), few DE algorithms such as population restart mechanisms (LaTorre and Peña, 2017), centroid-based population initialization (Salehinejad and Rahnamayan, 2016), and opposition-based learning (OBL) strategy in the shuffled differential evolution (SDE) (Ahandani and Alavi-Rad, 2012) use problem characteristics to divide the initial population into several subpopulations. Changing the population size is another aspect that DE algorithms can handle in static (Maučec and Brest, 2019) and dynamic fashions, which can be based on linear and non-linear population size-changing methods (Biswas and Suganthan, 2020; Tanabe and Fukunaga, 2014). Furthermore, some well-known DE algorithms (Tong et al., 2018; Wu et al., 2016) provide effective mechanisms to apply multi-populations to decrease the risk of stagnation risk.

Parameters setting: In the DE algorithms, specifying the scaling factor (F) and the crossover rate (CR) by appropriate values has a high impact on the performance, which remains a long-standing challenge. In the literature, this challenge has been handled primarily by either offline or online parameter settings. The algorithm designers set the values of the parameters in the offline methods before running the algorithm, and the values remain unchanged during the search process, whereas in the online parameter setting, the values of the parameters are adjusted in real-time. Concerning the philosophy of adopted online parameter settings, the DE variants can be classified into three classes: deterministic, adaptive, and self-adaptive (Eiben and Smith, 2015; Lu et al., 2020; Maučec and Brest, 2019). Some DE algorithms utilize deterministic rules to set the parameter values without getting any feedback (Eiben and Smith, 2015; Storn and Price, 1997), while SaDE (Qin and Suganthan, 2005), jDE (Brest et al., 2006), ADE (dos Santos Coelho et al., 2013), and SaNSDE (Yang et al., 2008) dynamically adapt the new values by getting feedback from the search process. The self-adaptation parameter setting is used in the SaMDE (Wang et al., 2013) DESAP (Zhong and Cai, 2015) and NAMDE

(Abderazek et al., 2019) algorithms, which can be adapted to different problems without any user interaction (Brest and Maučec, 2008).

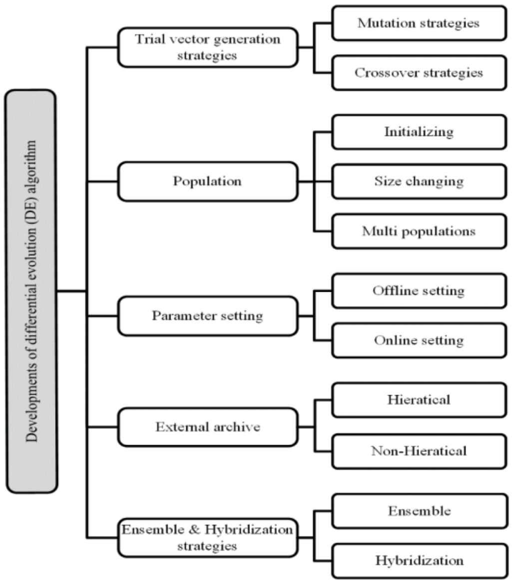

Fig. 1 Development of differential evaluation (DE) algorithms.

External archive: The DE algorithms use external archives with different characteristics in terms of structure and content to enhance population diversity. Meng et al. (Meng and Pan, 2019) proposed the HARD-DE algorithm, utilizing a new hierarchical archive to keep in-depth information of evolution to obtain a better perception of landscapes and improve the diversity of the trial vectors. Khanum et al. (Khanum et al., 2016) introduced the reflected adaptive differential evolution with two hierarchical external archives (RJADE/TA) to store superior solutions. Algorithms, such as JADE (Zhang and Sanderson, 2009), SHADE (Tanabe and Fukunaga, 2013), L-SHADE (Tanabe and Fukunaga, 2014), iLSHADE (Brest et al., 2016), LSHADE-EpSin (Awad et al., 2016b), and MPGDE (Yang et al., 2016), use a non-hierarchical memory to maintain success and inferior solutions and share their experiences.

Ensemble and hybridization strategies: Recently, ensemble methods have been actively pursued to design high-quality DE algorithms by employing multiple learning algorithms. Many differential evolution algorithms have been introduced in the literature to solve optimization problems using a pool of diverse strategies (Mallipeddi and Suganthan, 2010; Mallipeddi et al., 2011; Wu et al., 2016). In EPSDE (Mallipeddi et al., 2011), a pool of mutation strategies and corresponding control parameters coexists to compete throughout the evolution process and produce the trial vectors. The MTDE algorithm (Nadimi-Shahraki et al., 2020b) applies an adaptive movement based on a new multi-trial vector approach (MTV), which combines different search strategies. The EDEV algorithm (Wu et al., 2018) employs a multi-population based framework (MPF) to realize the ensemble of multiple DE variants. Both the multi-population ensemble DE (MPEDE) algorithm (Wu et al., 2016) and the improved version of MPEDE (IMPEDE) (Tong et al., 2018) provide a pool of diverse strategies for approximating the optimal global solution. Meanwhile, some DE algorithms (Awad et al., 2017; LaTorre et al., 2013) utilize a hybrid framework that enables them to combine several algorithms and increase the quality of the DE variants for solving complex optimization problems.

As mentioned above, much attention has been devoted to developing DE algorithms due to their abilities to solve a variety of optimization problems. Nevertheless, for solving complex problems, the DE algorithms suffer from weak local searchability, premature convergence, low diversity, among other weaknesses (Brest and Maučec, 2008; Cai and Wang, 2015; Mallipeddi and Suganthan, 2010; Mallipeddi et al., 2011; Maučec and Brest, 2019). Moreover, their performance deteriorates rapidly as the search space's dimensionality increases in the LSGO problems (Li et al., 2013; Maučec and Brest, 2019). The number of such complex and LSGO problems will continue to grow; therefore, it is an emerging issue to develop effective and scalable DE algorithms to solve the complex and LSGO problems. Then, extending the DE algorithms using multi-trial generation strategies appear to be a sufficient approach, since theoretically, no general optimization algorithm will be superior and answer these needs.

In this study, an effective and scalable DE algorithm, named quantum-based avian navigator algorithm (QANA), is proposed to solve the global optimization problems. The QANA is inspired by migratory birds' ability to navigate long-distance aerial paths with extraordinary precision using their quantum-based avian navigator and the communication topologies (Bajec and Heppner, 2009; Wang et al., 2006). The QANA is modeled and implemented by introducing two long-term and short-term memories to maintain diversification, a topology named V-echelon to share information and guide its flow, and quantum-based navigation including two mutation strategies and a qubit-crossover operator to move search agents toward better solutions. Initially, different geographic zones using random centroids are determined to form a number of flocks by randomly distributing search agents. Then, during the evolutionary process, the introduced success-based population distribution (SPD) policy assigns each flock using its previous success rate to one of the quantum-based navigation strategies through which the search agents are moved and exchanged information by the V-echelon communication topology. Meanwhile, the long-term (LTM) and short-term (STM) memories store the exploration experiences of search agents to maintain the diversity of the population. It is expected that the exploration of the search space by the flocks based on the SPD policy decreases the risk of stagnation since the majority of the population is assigned to the winner trial vector. Moreover, using the novel V-echelon communication topology can promote slow diffusion of unpromising information flow through the population by enhancing the population diversity and suspending premature convergence.

The effectiveness of the proposed QANA was experimentally evaluated by conducting the benchmark test functions, CEC 2018 (Awad et al., 2016a), with different dimensions, 30, 50, and 100. Moreover, the scalability of QANA was assessed by the benchmark test functions CEC 2013 (Li et al., 2013), with dimension 1000 as LSGO problems. In addition, four engineering problems were considered to evaluate the applicability of QANA to solve real-world problems. Statistically, the proposed algorithm was also analyzed by three statistical tests: Wilcoxon signed-rank sum, analysis of variance (ANOVA) and mean absolute error (MAE). The obtained results were further compared with well-known SI and DE variants to prove the superiority of the proposed QANA over other algorithms.

2. Inspiration

Bird migration is a remarkable natural phenomenon in which massive swarms of birds, such as robins and geese, migrate thousands of miles annually to find the best ecological conditions and habitats for feeding and breeding. In this extraordinary process, the question of origin concerns how the migratory birds navigate such long-distance aerial paths with extraordinary precision and without utilizing various cues, such as an atlas, GPS, or road signs during the migration (Mouritsen, 2018). Over the recent decades, ornithologist studies have demonstrated that the birds have an avian navigator equipped with quantum-based magnetoreception, which senses the Earth's magnetic field to determine their direction, altitude, and location (Wang et al., 2006; Zhang et al., 2015). Recent works have also revealed that the migratory birds enhance communication and coordination by aggregation into the flocks, and they have an interaction with different topologies to conserve much-needed energy during their lengthy and challenging flight (Wiltschko and Wiltschko, 2009). The quantum-based avian navigator and communication topologies of the migratory birds motivated us to investigate and develop a quantum-based avian navigator (QANA) algorithm.

Magnetoreception is a sense (magnetic compass) in the avian navigator that provides information about migratory birds' spatial navigation (Maeda et al., 2008; Mouritsen, 2018). This information is received by the receptor molecules in cryptochromes proteins located in the avian retina and is then transmitted to the optical nervous system for a meaningful reaction (Wang et al., 2006). As shown in Fig. 2(a), a quantum of light (a photon) enters a bird’s eye during migration and hits the retina, then this energy can excite the receptor molecules to produce unpaired electrons. The relative alignment of unpaired electrons exists in two states, singlet and triplet, which are affected by the interaction with Earth's magnetic field (Zhang et al., 2015). As shown in Fig. 2(b), after a photon hits the retina, two main actions occur in the avian navigator. First, the energy of the photon splits these two electrons. Then, depending on the bird's orientation concerning Earth's magnetic field, these two electrons are recombined, and their spin with two possibilities may or not remain in the quantum correlated (quantum entanglement) (Maeda et al., 2008; Wang et al., 2006). If the orientation is true, then the electrons stay entangled with opposite spins or in the singlet state through which they release the original energy of the photon, producing a stimulus to the optical nerve of the bird. If the orientation is wrong, then the spins end up parallel or in the triplet state, and the optic nerve of the bird does not receive the stimulus.

Commented [AHG1]: Or "correlation"?

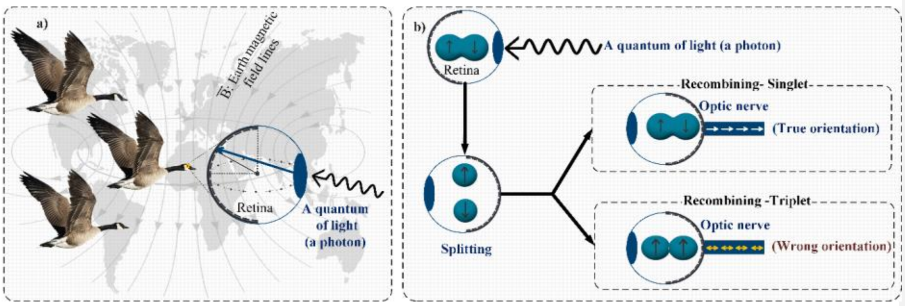

(a). The retina hitting (b). Two main actions, splitting and recombining (quantum entanglement)

Fig. 2 The process of providing information about spatial navigation by an avian navigator.

As shown in Fig. 3, the migratory birds exhibit orderly aerial maneuvers using V-echelon topology. This flight formation conserves their flight energy efficiency by taking advantage of the upwash vortex fields created by the birds' wings in front and facilitating the orientation and communication among the birds during their long, arduous migration (Mouritsen, 2018). The V-echelon formation and its advantages inspired us to introduce a novel communication topology in this study.

3. Avian navigator modeling

Motivated by the above inspiration, we modeled the avian navigator by introducing quantum-based navigation, including two new mutation strategies and a qubit-crossover operator, to move the search agents using a communication topology and two long-term and short-term memory structures. In our model, these mutation strategies are equipped with a quantum orientation mechanism to produce their trial vectors. Each quantum-based mutation strategy utilizes the introduced V-echelon topology in which the search agents communicate and share the information of the promising solutions generated during the optimization process. This presented communication topology can increase the diversification and exploration ability of navigation strategies, which significantly impact our avian navigator's performance.

Suppose Avian = $\{a_1, a_2 \ldots a_N\}$ is a finite set of N distinct migratory birds or search agents randomly distributed equally in k different geographic zones determined by random centroids.

The position of search agent a_i in the current iteration t is denoted by $X_i(t) = [x_{i1}, x_{i2} \dots x_{iD}]$, which is a feasible solution to the corresponding problem in a D-dimensional search space. This distribution forms k flocks, each including n search agents, where n=N/k. In each iteration, each flock's search agents explore the search space by using one of the quantum-based mutation strategies selected by the success-based population distribution (SPD) policy. The visited aerial paths' specifications are archived by the long-term and short-term memories to provide meaningful knowledge for partial landscape analysis. The structure of these memories, V-echelon communication topology, and quantum-based navigation are described in the following sections.

3.1. Long-term and short-term memories

Migratory birds regularly remember the visited landscapes and aerial paths during their navigation to utilize information kept in their memory. Motivated by this ability, we define long-term memory (LTM) and short-term memory (STM) strategies.

Definition 1 (Long-term memory): Let LTM= $\{LTM_1, LTM_2, \dots, LTM_i, \dots, LTM_N\}$ be a finite set of N distinct memories. The LTM_i is the long-term memory of the search agent a_i to archive its superior solutions gained during the optimization process. The LTM_i is filled by positions $\{X_1, \dots, X_j, \dots, X_{Ҡ'}\}$, where Ҡ' is the memory size, and $X_j = \{x_{j1}, x_{j2}, \dots, x_{jD}\}$. The vector X_1 is the position of a_i once the population is distributed in the search space. In the LTM_i, $F(X_j) < F(X_{j-1})$, where F is the fitness function, and in each iteration, the position of a_i is maintained by its long-term memory LTM_i if the fitness of this position is less than the last member of the LTM_i. Whenever the memory size of LTM_i is completed, a new solution is replaced with its nearest existing solution found by the Euclidean distance because the new solution dominates its neighbors.

Definition 2 (Short-term memory): Consider a finite set of STM = $\{X_1, \dots, X_j, \dots, X_{Ҡ''}\}$ as a short-term memory with memory size Ҡ''. This is a global memory for the population to keep the inferior positions generated by all search agents. After distributing the population in the search space, STM is initialized by Ҡ'' inferior positions of the population. Then, at the end of each iteration, the worst Ҡ'' inferior positions gained during this iteration are completely replaced with the current members of the STM.

3.2. V-echelon communication topology

Inspired by migratory birds' navigation behaviors, we modeled their flight formation to spread the information flow throughout the search agents by introducing V-echelon communication topology. In the following, the V-echelon topology is defined based on its properties.

Definition 3 (V-echelon topology): Let V be a set of n members of the flock f_q, including a header (H) and two subsets denoted right-line (R) and left-line (L), which are considered in a V-shaped formation, as shown in Fig. 3(a). Then, V is a V-echelon topology if it satisfies the following properties, where X_s is a representative set of n members of the flock f_q, and F is the fitness function.

Property V1: $X_s = \{X_i \mid X_i \in fq,\ 1 \leq i \leq n,\ F(X_i) \leq F(X_{i+1})\}$.

Property V2: The header H, as the leader of V, is the best member of X_s, then $H = X_1$.

Property V3: The rest of the representation set X_s (X_s – H) forms two subsets, right-line (R) and left-line (L) such that $R = \{X_{2j} \mid X_{2j} \in X_s,\ 1 \leq j \leq n/2\}$ and $L = \{X_{2j+1} \mid X_{2j+1} \in X_s,\ 1 \leq j \leq n/2\}$.

Property V4: In the V, each member of R and L is computed by following its front member in these lines such that in the right-line, $X_{2j+2} = M(X_{2j})$, and in the left-line, $X_{2j+3} = M(X_{2j+1})$ where M can be provided by different mutation functions to compute the position of $X_i \in X_s$ and $1 \leq j \leq n/2$. Consistently, both front members of R and L subsets follow H ($X_2 = M(H)$ and $X_3 = M(H)$). Fig. 3(b) shows the schematic structure used for a V-echelon topology.

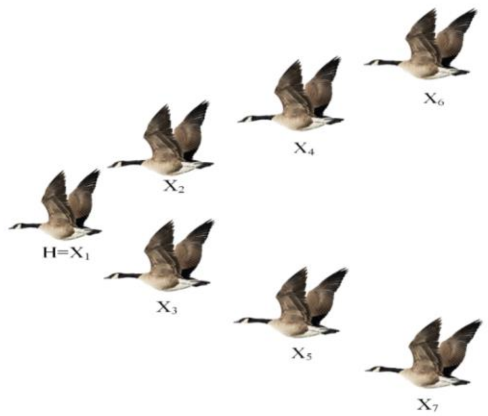

Fig. 3(a) The V-shaped formation consisting of a header (H) and two subsets, right-line (R) and left-line (L).

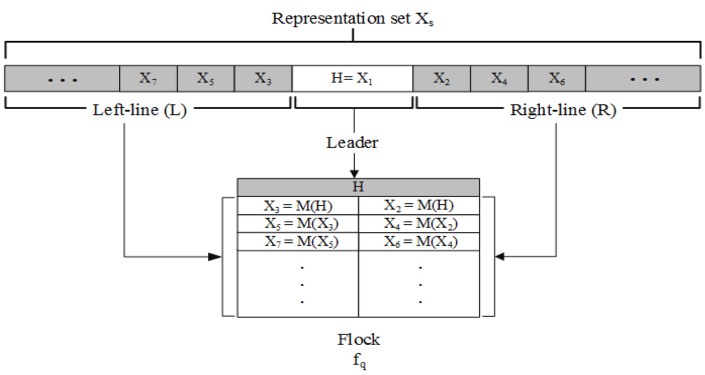

Fig. 3(b) The schematic structure of V-echelon topology.

Fig. 3 V-echelon communication topology.

3.3. Quantum-based navigation

The flocks explore the search space using the introduced quantum-based navigation, including success-based population distribution (SPD) policy, two new mutation strategies, "DE/quantum/I" and "DE/quantum/II," and a qubit-crossover operator. During the optimization process, each flock is assigned one of these mutation strategies based on the SPD policy defined in Definition 4.

Definition 4 (SPD policy): The success-based population distribution (SPD) policy assigns the flocks to the mutation strategies dynamically based on their improvement rate. The success rate of mutation strategy M_m is denoted by SR_m and computed by Eq. (1), where f_m is the set consisting of flocks that use M_m in iteration t, and τ_{ij} is equal to 1 if M_m could improve a_j of i-th flock of the set f_m, otherwise, τ_{ij} is equal to 0.

$$SR_m(t) = ((\sum_{i\in f_m} \frac{\sum_{j=1}^{n} \tau_{ij}}{n})/|f_m|) \times 100 \tag{1}$$

In the first iteration, each flock is randomly assigned by one of the quantum mutation strategies. Then, in each iteration t, each quantum mutation strategy's success rate is computed by Eq. (1) to determine the winner mutation strategy. The SPD policy rewards the winner mutation strategy by assigning it to the majority of flocks in the iteration t+1. It is expected that this SPD policy can decrease the risk of stagnation since a greater success rate is gained by the winner trial vector.

Quantum mutation strategies: The quantum-based navigation introduced in our modeling consisted of two quantum mutation strategies, DE/quantum/I and DE/quantum/II, defined by Eqs. (2) and (3), respectively, where x_i (t) is the position of search agent a_i in the current iteration t, $\hat{x}_{V\_echelon}(t)$ is the position of the search agent followed by a_i based on Definition 3 of v-echelon topology, $\hat{x}_{j\in STM}(t)$, $\hat{x}_{j\in LTM}(t)$ are positions that are randomly selected from STM and LTM memories, respectively, and x_{best} (t) is the position of the best search agent. The parameter $S_i(t)$ is a self-adaptive quantum orientation that is defined by Definition 5. The trial vector v_H (t+1) as a leader in the V-echelon topology is determined using Eq. (4), where the parameters L and U are the lower and upper bound of the search space, respectively.

$$v_i(t+1) = x_{best}(t) + S_i(t) \times \left(\hat{x}_{V_{echelon}}(t) - \hat{x}_{j\in LTM}(t)\right) + S_i(t) \times \left(\hat{x}_{V\_echelon}(t) - x_{best}(t)\right) + S_i(t) \times \left(\hat{x}_{j\in LTM}(t) - \hat{x}_{j\in STM}(t)\right) \tag{2}$$

$$v_i(t+1) = S_i(t) \times \left(x_{best}(t) - \hat{x}_{V_{echelon}}(t)\right) + S_i(t) \times \left(x_i(t) + \hat{x}_{j\in LTM}(t) - \hat{x}_{j\in STM}(t)\right) \tag{3}$$

$$v_H(t+1) = S_i(t) \times x_{best} + (\mathrm{L} + (\mathrm{U} - \mathrm{L}) * rand(0.1)) \tag{4}$$

Definition 5 (Self-adaptive quantum orientation): Let the quantum orientation S_i (γ) for avian a_i be defined by Eq. (5) (Wang et al., 2006) as a sensitivity of the receptor molecules containing radical pairs that have an angle of γ with Earth's magnetic field. In this equation, the parameter $\mathcal{L}_S$ is the weighted Lehmer mean (Tanabe and Fukunaga, 2013) that is computed by Eq. (7); the parameter $\Phi_{Si}(\gamma)$ is the singlet yield corresponding to the angle γ that is computed by Eq. (6) (Wang et al., 2006); and the parameter $\bar{\Phi}_{Si}(\gamma)$ is the average singlet yield over all angles. In Eq. (6), the parameter k is the decay rate, γ_e is the electron gyromagnetic ratio, and B is the magnetic field intensity.

$$S_i(\gamma) = \mathcal{L}_S + rand(0.1) \times (\Phi_{Si}(\gamma) - \bar{\Phi}_{Si}(\gamma)) \qquad 0 \le \gamma < 2\pi \tag{5}$$

$$\Phi_{Si}(\gamma) = \frac{6k^2+5\times(\gamma_e\times B)^2+(\gamma_e\times B)^2\times\cos(2\gamma)}{16(k^2+(\gamma_e\times B)^2)} \qquad k = 0.3, \gamma_e = rand, B = 1.76085 \tag{6}$$

$$\mathcal{L}_S = \frac{\sum_{S_i\in\hat{S}} w_{S_i} \times S_i^2}{\sum_{S_i\in\hat{S}} w_{S_i} \times S_i} \tag{7}$$

In Eq. (7) $\hat{S}$ is the set of successful self-adaptive quantum orientations S_i that F (U_i (t+1)) < F (X_i (t)) where 1 ≤ i ≤ N, and the parameter w_{S_i} is the weighting factor of S_i that is calculated by Eq. (8).

$$w_{S_i} = \frac{|F(U_i(t+1)-F(X_i(t))|}{\sum_{i=1}^{|\hat{S}|}|F(U_i(t+1)-F(X_i(t))|} \tag{8}$$

Qubit-crossover operator: The mutant vector v_i(t+1) is crossed by its parent x_i(t) in order to generate trial vector u_i(t+1) using Eq. (9), where, $|\psi_i\rangle_d$ is a qubit-crossover probability of dimension d-th that is defined by Definition 6.

$$u_{id}(t+1) = \begin{cases} v_{id}(t+1) & |\psi_i\rangle_d \ge rand \\ x_{id}(t+1) & |\psi_i\rangle_d < rand \end{cases} \tag{9}$$

Definition 6 (Qubit-crossover probability): Given $|\psi_i\rangle$ as a qubit-crossover probability for the search agent $a_{i,}$, which is a two-state quantum system denoted by $|0\rangle = \binom{1}{0}$ and $|1\rangle = \binom{0}{1}$ (Nielsen and Chuang, 2001). In each iteration, for each dimension of the trial vector u_i(t+1), a qubit-crossover $|\psi_i\rangle_d$ is computed by Eq. (10), which is visualized by Fig. 4 using a Bloch sphere (Nielsen and Chuang, 2001), and the probability $|\psi_i\rangle_d$ is considered a final solution. In this equation, the parameter $|\psi_R\rangle_d$ is a random distribution, which is coefficient for changing the length of the vector $|\psi_i\rangle_d$ in the Bloch sphere.

$$|\psi_i\rangle_d = |\psi_R\rangle_d \times \left(cos\left(\frac{\theta}{2}\right)|0\rangle + e^{i\varphi}\, sin\left(\frac{\theta}{2}\right)|1\rangle\right) \qquad \theta,\ \varphi = rand \times \frac{\pi}{2} \tag{10}$$

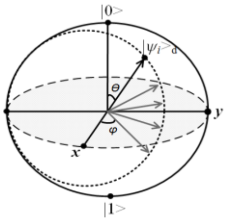

Fig. 4 Visualizing a qubit-crossover probability $|\psi_i\rangle_d$ using the Bloch sphere (Nielsen and Chuang, 2001).

4. QANA

This section proposes a novel evolutionary algorithm denoted the quantum-based avian navigator algorithm (QANA) based on the avian navigator modeling introduced in the previous section. In the following section, the QANA's step-wise procedure is summarized, and its pseudo-code is shown in Fig. 5.

```
Algorithm: Quantum-based avian navigator algorithm (QANA)
Input: N (number of search agents), k (number of flocks), and MaxIt (maximum iterations).
Output: The global best solution.
Begin
Initialization.
Set t = 1.
While t ≤ MaxIt
    Constructing k flocks.
    Set long-term and short-term memories using Definitions1and 2.
    Forming the V-echelon communication topology of each flock using Definition 3.
    Assigning each flock to a mutation strategy using the SPD policy defined by Definition 4.
    For q = 1→ k
        For i = 1→ N/k
            Generating the mutant vector v_i(t+1) for each search agent a_i of flock f_q using Eqs. (2- 4).
            Crossover the mutant vector v_i(t+1) to generate trial vector u_i(t+1) using Eq. (9).
            If F(U_i (t+1)) ≤ F(X_i (t))
                X_i (t+1) = U_i (t+1).
            Else
                X_i (t+1) = X_i (t).
            End If
        End For
    End For
    t = t + 1.
End while
Return the position of the best search agent as a global best solution.
End
```

Fig. 5 The pseudo-code of the proposed quantum-based avian navigator algorithm (QANA).

Step 1. Initialization: Set N distinct migratory birds or search agents that are randomly distributed in k different geographic zones determined by k random centroids.

Step 2. Flock construction: Construct k flock by selecting n=N/k search agents randomly form the population for each flock.

Step 3. Set long-term and short-term memories: Set the LTM for each search agent using Definition 1 and STM for all search agents using Definition 2.

Step 4. V-echelon topology formation: Forming the communication topology of each flock using Definition 3, as shown in Fig. 3.

Step 5. Mutation strategy assigning: Assign each flock to a mutation strategy using the SPD policy defined by Definition 4.

Step 6. Trial vector generation: Generate the trial vector of each search agent a_i of flock f_q using its assigned mutation strategy by Eqs. (2-4).

Step 7. Crossover: Crossover the mutant vector $v_i(t+1)$ by its parent $x_i(t)$ in order to generate trial vector $u_i(t+1)$ using Eqs. (9) and (10).

Step 8. Selection: Compare the fitness values of each trial vector $F(U_i(t+1))$ with its corresponding target vector $F(X_i\ (t))$, and select the dominant trail vector.

Step 9. Algorithm termination: Stop the algorithm if the termination criterion is satisfied; otherwise jump to step 2 to repeat the search process for more favorable solutions in a specific problem.

5. Experimental evaluation of the QANA

A variety of experiments were designed to evaluate the performance of the QANA. These experiments are set up differently to analyze the QANA's behaviors to reflect its qualitative and quantitative aspects. First, a qualitative analysis was performed based on four metrics, including search history, trajectory, average fitness values, and convergence rate, to show the proposed algorithm's exploration and exploitation abilities and its convergence behavior for solving problems. Then, in the quantitative analysis, the effectiveness and scalability of the proposed QANA were compared with other competitive algorithms. The effectiveness was evaluated by testing the exploitation and exploration, escape ability from local optima, and convergence speed, while the scalability was assessed by solving LSGO problems. Due to the stochastic nature of the optimization algorithms, the overall performance of the algorithms was statistically analyzed by three non-parametric statistical tests, i.e. Wilcoxon signed-rank sum, analysis of variance (ANOVA), and mean absolute error (MAE). The applicability of the QANA for real-world optimization problems was also assessed by solving four engineering design problems.

The QANA was coded using Matlab version R 2016b programming language, and to ensure a fair comparison, all competitor algorithms were also run under the same conditions in this Matlab version. All experiments were run using the same configuration, including an Intel(R) Core(TM) i7 CPU with 3.4 GHz and 8 GB memory on Windows 7 operating system.

5.1. Benchmark test functions

Due to the theoretical limitations, the performance verification of a new metaheuristic algorithm is difficult. Thus, several benchmark functions, such as the CEC test suite in which the complexity degrees deteriorate rapidly as the dimensionality increases (Li et al., 2013;

Maučec and Brest, 2019; Sun et al., 2018; Zamani et al., 2019), have been introduced to evaluate the effectiveness and scalability of new metaheuristic algorithms. Therefore, the effectiveness of the proposed QANA was tested by benchmark functions CEC 2018 (Awad et al., 2016a) with different dimensions 30, 50, and 100, and its scalability was evaluated using CEC 2013 (Li et al., 2013) with dimension 1000.

The CEC 2018 test suite consists of four groups: unimodal, simple multimodal, hybrid, and composition. Functions (F_1 and F_3) are unimodal test functions with one global optimum with non-separable, symmetric, and smooth properties but a narrow ridge, so they are suitable for evaluating the proposed algorithm in terms of the exploitation ability and convergence speed. In the second group, there are seven multimodal functions (F_4–F_{10}), which have many local optima that are mostly used to test the exploration ability and local optima avoidance of the QANA. Besides, functions (F_{11}– F_{20}) and (F_{21}–F_{30}) of the third and fourth groups are hybrid and composition, respectively, that are more complex and challenging than unimodal and multimodal functions. Due to their more rugged nature and ability to maintain continuity around the global optima, these functions are suitable for testing the balance between the exploration and exploitation abilities and premature convergence. Also, the search space's bounds for all of the functions were limited between interval $[-100, 100]^D$, where D is the dimension of the corresponding problems.

Moreover, the CEC 2013 benchmark suite (Li et al., 2013) consists of fifteen test functions: fully-separable functions (F_1–F_3), partially additively separable functions (F_4–F_{11}), overlapping functions (F_{12}–F_{14}), and non-separable function (F_{15}) with different properties, which are suitable to test the scalability. In the CEC 2013, all functions were used with dimension 1000, except functions F_{13} and F_{14} in which the dimension was 905. Moreover, the bounds of the search space were set differently, such that they were limited between interval [-100, 100] for functions F_1, F_4, F_7, F_8 and F_{11}–F_{15}, between interval [-5, 5] for functions F_2, $F_{5,}$ and F_9, and between interval [-32, 32] for functions F_3, F_6 and F_{10}.

5.2. Qualitative analysis

In this subsection, the qualitative behavior of QANA is analyzed in terms of convergence, population diversity, and exploration and exploitation. These analytical experiments were performed by 60 search agents distributed equally in 4 flocks on a 2-dimensional search space on some functions with different properties selected from the CEC 2018.

Commented [ns2]: Consider: by distributing 60 search agents equally in 4 flocks..

5.2.1. Convergence analysis

The convergence behavior of QANA was analyzed using four metrics, including search history, average fitness values, best fitness values, and trajectory, which are plotted in the second to fifth columns of Figs. 6 and 7, respectively. Their respective landscapes are also presented in the first column of these figures.

The search history of all search agents is tracked along the contour lines with a solid black circle, and the global optimum solution is marked with a red star. This experiment shows the movement history of search agents during the evolutionary process for finding the global optimum solution. The third column displays the QANA's ability to improve the candidate solutions by computing the average fitness values in each iteration. Then, the globally best values obtained during the optimization are shown in the fourth column, revealing the convergence ability of the QANA. Finally, the fifth column shows the trajectory in which the first dimension of the representative search agent a_1 is tracked to show how the proposed algorithm has abrupt movements in the initial iterations for exploration and gradually converges to a region in the final iterations for exploitation.

The search history results show that the QANA follows the same pattern on all of the test functions. In the unimodal test function F_1, the search agents bypass the local optima with a long step size to reach the promising region and exploit in the vicinity of the global optimum very precisely. In test functions, F_6 and F_{10}, the landscape composed of many basins of attraction and the behavior of the QANA show that it is able to move out the basin from a given local optimum and approximate the region of a global optimum effectively. As shown in the first column in Figs. 6 and 7, the landscapes of the hybrid and composition test functions F_{21}–F_{28} are composed of numerous deep valleys, which simultaneously benchmarked the ability of exploration and exploitation and the local optima avoidance of the proposed algorithm. These observations concluded that the introduced movement strategies are able to bypass the deep valleys efficiently and approximate the global optimum of optimization problems.

Commented [ns3]: Changed to landscapes

The results were evaluated based on the average fitness values. The results prove that the QANA can evolve the obtained candidate solutions towards a global optimum solution for different landscapes. In the test functions F_1, F_6, and F_{10}, the proposed algorithm has an accelerated convergence trend toward the global optimum with the steepest descent slope. In the challenging test functions F_{21}–F_{28}, the proposed algorithm can discover the optimum solution in a slight slope. It initially analyzes the search space by exploring and bypassing the local optima, contributing to the promising regions using its exploitability. The trajectory curves plotted in the fifth column demonstrate that the representative search agent a_1 starts its evolutionary process with the abrupt changes at the initial iterations, then gradually decreases as it becomes closer to the solution over the course of iterations. This behavior guarantees that the proposed algorithm eventually converges to a point in the landscape.

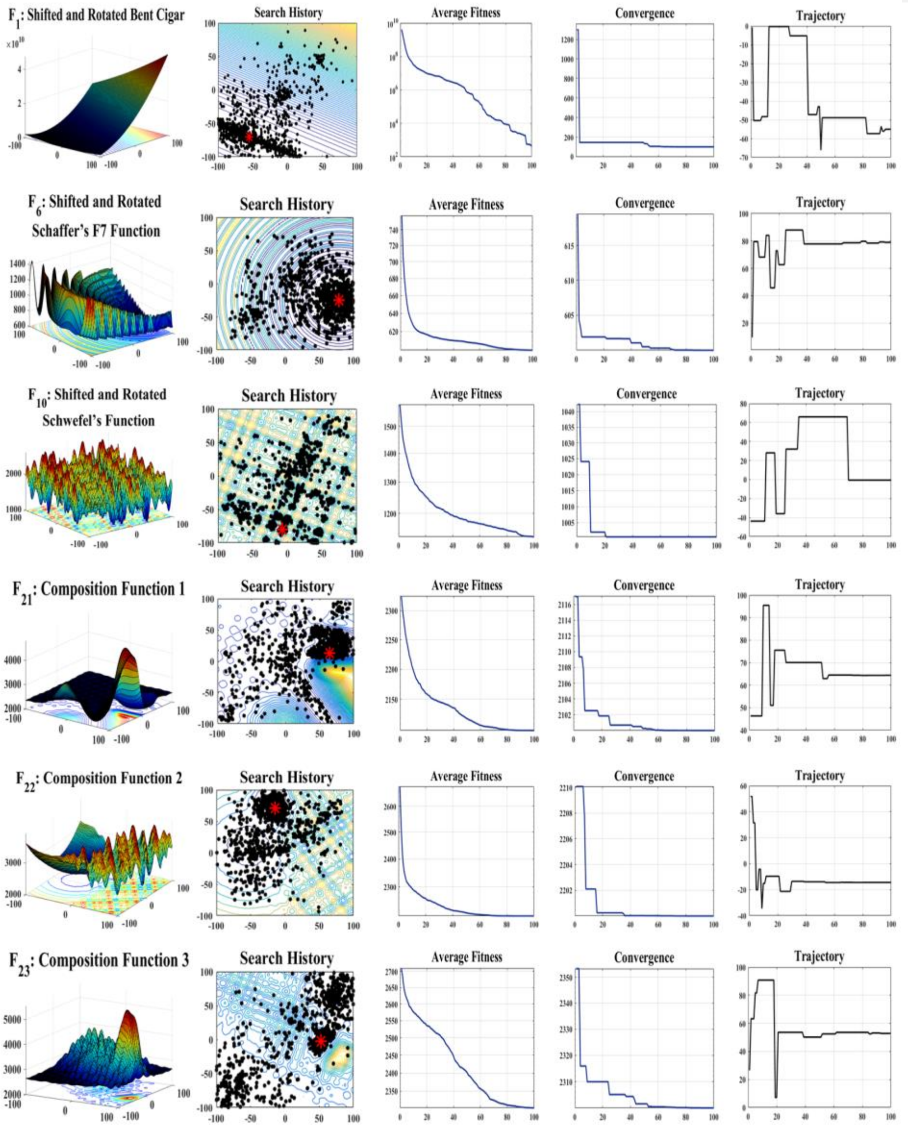

Fig. 6 Search history, average fitness, convergence curve, and trajectory in the first dimension of QANA.

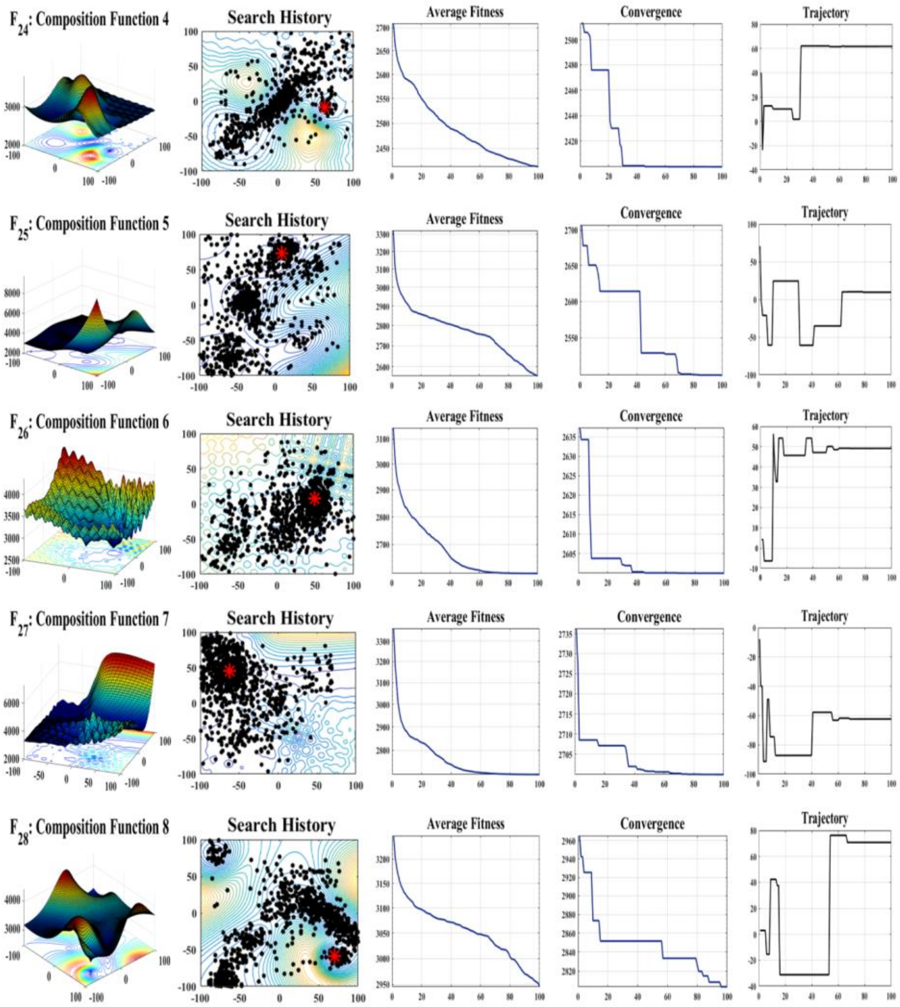

Fig. 7 Search history, average fitness, convergence curve, and trajectory in the first dimension of QANA.

5.2.2. Population diversity analysis

Population diversity maintenance during the search process is an essential attribute that can prevent or suspend the search agents from the local optima trapping. Increasing the dimensionality results in the population dispersion which prematurely converge to the unpromising areas throughout iterations. In this subsection, the proposed QANA algorithm's population diversity was analyzed in different dimensions, 30, 50, and 100. The obtained results for some of the test functions are plotted in Fig. 8. The population diversity was computed using Eq. (11) (Olorunda and Engelbrecht, 2008), where the parameter N is the number of search agents, D is the dimensionality of the problem, x_{id} is the position of i-th search agent in d-th dimension, and $\overline{x_d}$ is the average of d-th dimension.

$$D = \frac{1}{N}\sum_{i=1}^{N}\sqrt{\sum_{d=1}^{D}(x_{id} - \overline{x_d})^2} \tag{11}$$

In these curves, a small value indicates the population convergence, while a large value reveals a higher population dispersion. The curves show that the QANA algorithm can maintain population diversity for different test functions of unimodal, multimodal, hybrid, and composition with dimensions of 30, 50, and 100.

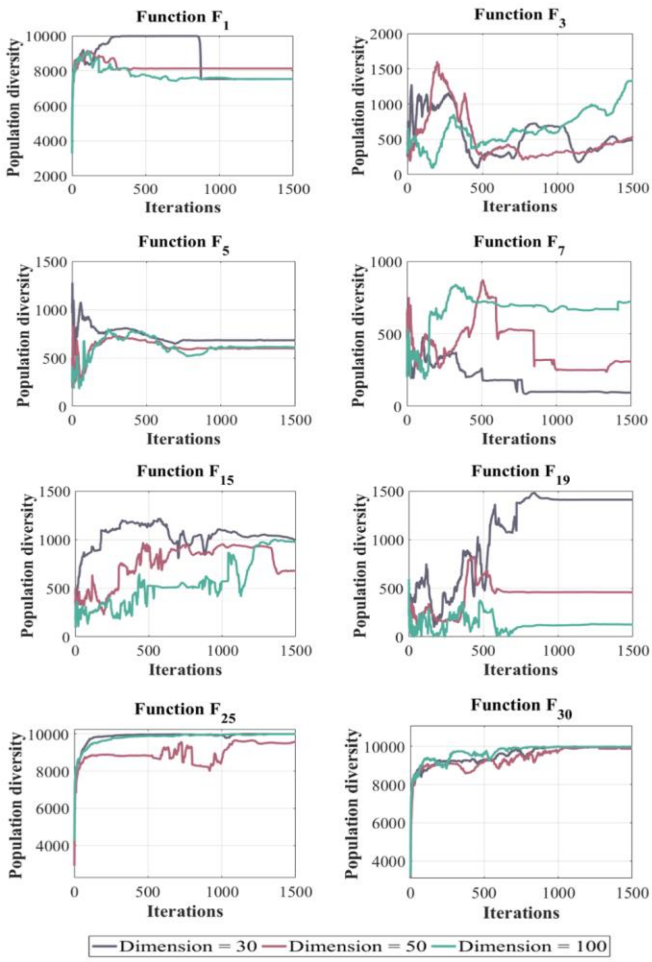

Fig. 8 Population diversity analysis of QANA in unimodal, multimodal, hybrid, and composition test functions.

5.2.3. Exploration and exploitation analysis

In this experiment, the exploration and exploitation abilities of the proposed QANA algorithm in the face of different problems with various properties, such as unimodal, multimodal, hybrid, and composition, were analyzed. The obtained results are plotted in Fig. (9) to show the exploration and exploitation percentage during the evaluation process for different dimensions, 30, 50, 100, and 1000. A high percentage of exploration shows the considerable distance among search agents for finding the unvisited areas. Meanwhile, the high percentage of exploitation shows that the population's distance decerases and converges to the promising area. Thus, the balance between exploration and exploitation can suspend the premature convergence and alleviate the loss of diversity (Hussain et al., 2019).

The percentages of exploration and exploitation during the search process were computed using Eqs. (12) and (13) (Hussain et al., 2019). The parameter Div (t) is computed using Eq. (14) to show the increase and decrease of distance among search agents, and Div_{max} is the maximum diversity in the entire iterations. In Eq. (14), parameter x_{id} (t) is the position of i-th search agent in the d-th dimension, and x_d (t) is the median value of the d-th dimension for all N search agents, respectively.

$$Exploration\ (\%) = \frac{Div(t)}{Div_{max}} \times 100 \tag{12}$$

$$Exploitation(\%) = \frac{|Div(t) - Div_{max}|}{Div_{max}} \times 100 \tag{13}$$

$$Div(t) = \frac{1}{D}\sum_{d=1}^{D}\frac{1}{N}\sum_{i=1}^{N}|median\{x_d(t)\} - x_{id}\ (t)| \tag{14}$$

These curves show that the proposed QANA algorithm can strike balance between exploration and exploitation and find the near-optimal solution for different problems.

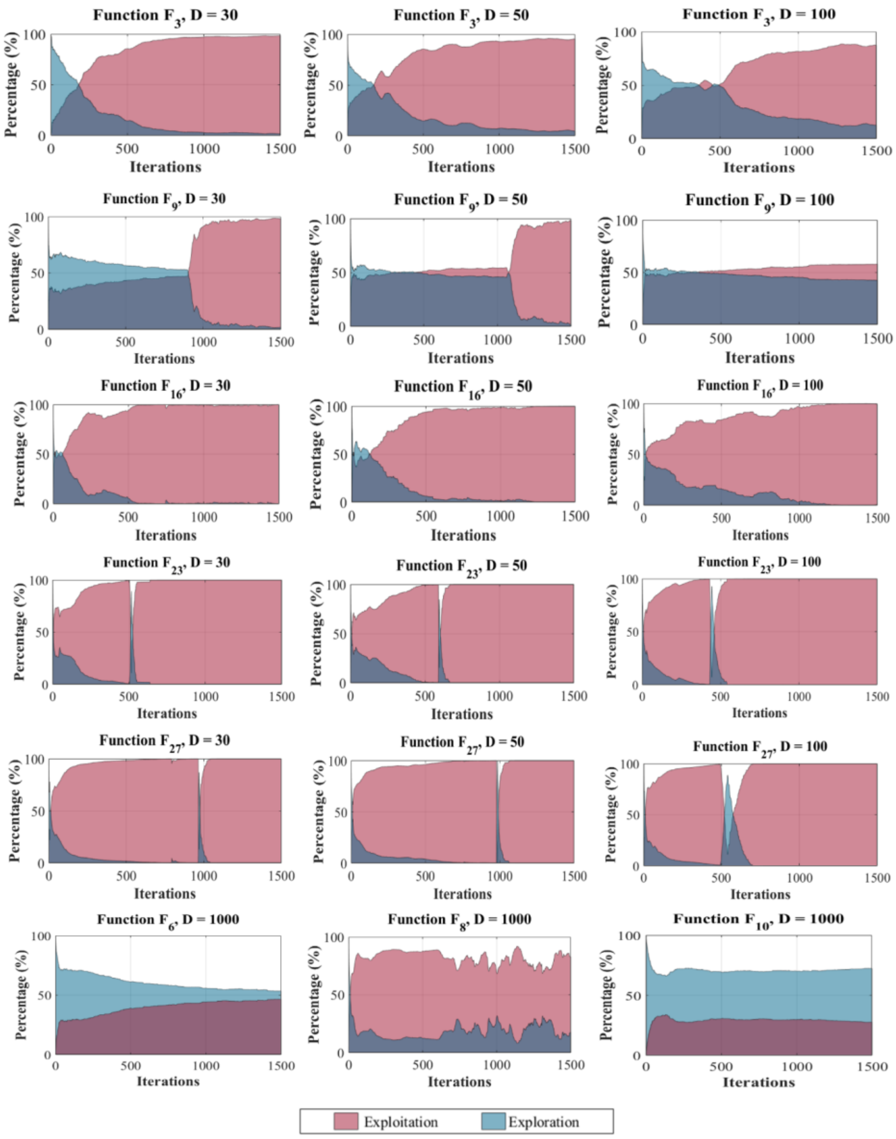

Fig. 9 Exploration and exploitation analysis of QANA.

5.3. Quantitative analysis

In the quantitative analysis, the proposed QANA was compared with several state-of-the-art algorithms, including DE variants, self-adapting control parameters in differential evolution (jDE) (Brest et al., 2006), hybrid differential evolution with biogeography-based optimization (DE/BBO) (Gong et al., 2010), differential evolution with composite trial vector generation strategies and control parameters (CoDE) (Wang et al., 2011), Sanskrit word meaning victory (Jaya) (Rao, 2016), monkey king evolutionary (MKE) (Meng and Pan, 2016), and weighted differential evolution algorithm (WDE) (Civicioglu et al., 2020), and SI algorithms such as salp swarm algorithm (SSA) (Mirjalili et al., 2017), exploration-enhanced grey wolf optimizer (EEGWO) (Long et al., 2018), modified whale optimization algorithm (MWOA) (Sun et al., 2018), and arithmetic optimization algorithm (AOA) (Abualigah et al., 2021). The effectiveness of the QANA was evaluated by conducting the CEC 2018 benchmark suite in terms of exploitation and exploration abilities, local optima avoidance, and convergence. Moreover, the scalability of the proposed algorithm was also analyzed using CEC 2013 with dimension 1000 as large-scale global optimization problems (Li et al., 2013). In all quantitative experiments, the initial parameters of the competitor algorithms were set according to the original papers, as shown in Table 1. Moreover, the values of the common parameters, such as population size (N) and maximum function evaluations (MaxFEs), were set to 200 and D×10000, respectively. Due to the random nature of the algorithms and to achieve a more comprehensive comparison, all quantitative experiments and statistical tests were run 30 times over the benchmark functions.

The experimental results are tabulated in Tables 2–4, where Avg, SD, and Min are the mean, standard deviation, and minimum fitness value, respectively. The best result for each function is highlighted and in boldface, and the comparisons are shown at the end of each table based on the numbers of the win (W), tie (T), and loss (L) of each algorithm.

5.3.1 Evaluation of exploitation and exploration

The exploitation and exploration abilities of the QANA were benchmarked against the contender algorithms using the unimodal and multimodal functions. Since the unimodal functions, F_1 and F_3, have only one global optimum, they can assess the exploitation ability. The results reported in Table 2 for using these functions with different dimensions (30, 50, and 100) show that the QANA provides a very competitive exploitation ability. The main reason is that using the introduced V-echelon communication topology defined by Definition 3 spreads the information flow of good solutions using the representative set X_s, thereby boosting the exploitation ability.

The multimodal test functions, F_4–F_{10}, were considered for evaluating the exploration ability due to having a complex landscape with very rugged regions and multiple local optima. The obtained results from this evaluation show a good exploration ability. This is mainly because of exploring the landscape by multi-flocks which are constructed and then dynamically assigned in each iteration to the mutation strategies based on their improvement rate and the SPD policy defined in Definition 4. Using the qubit-crossover operator defined in Eq. (9) enhances the diversity, which can also improve the exploration ability of the QANA.

Table 1 The parameter settings of algorithms.

Algorithms	Parameters values
jDE	F= 0.5, CR = 0.9, τ_1 and τ_2 = 0.1.
DE/BBO	I = E = 1, π_{max} = 0.005, K = 2, scaling factor F = rand (0.1, 1), and crossover probability (CR) = 0.9.
CoDE	CR = [0.1, 0.9, 0.2], and F = [1, 1, 0.8].
Jaya	No parameter for initial setting.
MKE	FC = 0.7.
SSA	l=2, c_2, c_3 = random numbers in the interval [0, 1].
EEGWO	b_1 = 0.1, b_2 =0.9, non-linear modulation index μ=1.5, an initial= 2 and a final = 0.
WDE	There are no parameters other than the common parameters.
MWOA	b =1, the values of parameters p, r_1 and r_2 are a random number between interval [0, 1], $0 < \beta \leq 2$.
AOA	α = 5, μ= 0.5.
QANA	The number of flocks (k) = 10. K' = 9, Ќ"=50.

5.3.2 Evaluation of local optima avoidance

The evaluation of the local optima avoidance ability is a complex and challenging test that requires solving different problems. Therefore, the hybrid and composition benchmark functions F_{11}–F_{20}, and F_{21}–F_{30} that have other properties are suitable for evaluating the local optima avoidance's ability. Tables 3 and 4 show the results for solving the hybrid and composition test functions with dimensions 30, 50, and 100. The results prove that the proposed algorithm is very competitive to other algorithms and can accurately approximate the global optima solutions in the hybrid and composition problems for different dimensions. Thus, the proposed QANA can strike a balance between exploration and exploitation. The main reasons are that the proposed algorithm uses two different mutation strategies that can handle hybrid and composition problems while utilizing the introduced long-term and short-term memories in Definitions 1 and 2, which maintain the diversity.

Table 2 Comparison of optimization results obtained from unimodal and multimodal test functions.

Func.	D	Metrics	jDE (2006)	DE/BBO (2010)	CoDE (2011)	Jaya (2016)	MKE (2016)	SSA (2017)	EEGWO (2018)	WDE (2018)	MWOA (2018)	AOA (2021)	QANA
F_1	30	Avg	6.4769E+10	1.03844E+02	1.06172E+02	3.1458E+10	1.00022E+02	4.5079E+03	5.5092E+10	1.1751E+09	2.5512E+10	4.0204E+10	1.0000E+02
		SD	1.4030E+10	1.42898E+00	1.61947E+00	6.2989E+09	1.90931E-02	5.2536E+03	5.8141E+09	2.0186E+08	8.1351E+09	6.1158E+09	1.0220E-14
		Min	7.2406E+09	1.01664E+02	1.03247E+02	2.0129E+10	1.00003E+02	1.9447E+02	4.0603E+10	8.0520E+08	1.0534E+10	2.8769E+10	**1.0000E+02**
	50	Avg	1.2800E+11	1.90408E+03	2.05014E+03	8.3942E+10	1.52133E+02	7.5172E+03	1.0966E+11	4.5173E+09	5.8918E+10	9.8217E+10	1.0030E+02
		SD	1.8514E+10	1.75908E+03	1.37145E+03	1.0066E+10	5.69634E+01	9.7270E+03	6.7506E+09	5.6447E+08	1.1658E+10	9.3012E+09	1.2850E+00
		Min	4.8465E+10	1.79040E+02	4.17062E+02	7.1728E+10	1.01256E+02	2.0473E+02	9.1619E+10	3.1522E+09	3.3415E+10	7.6918E+10	**1.0000E+02**
	100	Avg	3.8935E+11	1.66217E+04	1.00962E+03	2.2982E+11	2.60746E+02	1.1492E+04	2.6711E+11	1.8535E+10	1.7548E+11	2.6239E+11	1.0020E+02
		SD	1.8623E+10	8.63675E+03	4.47651E+02	2.9327E+10	3.27224E+02	1.1585E+04	6.6847E+09	1.9963E+09	1.4939E+10	1.1541E+10	4.0400E-01
		Min	3.5015E+11	2.59544E+02	3.58430E+02	1.8100E+11	1.02349E+02	1.6432E+02	2.5239E+11	1.3868E+10	1.3880E+11	2.3598E+11	**1.0000E+02**
F_3	30	Avg	1.0072E+05	6.70028E+04	3.00773E+02	2.3632E+05	2.63582E+04	3.0000E+02	8.8657E+04	8.0510E+04	8.0821E+04	7.3776E+04	3.0000E+02
		SD	1.6696E+04	8.02561E+03	2.99105E-01	3.7484E+04	5.66511E+03	1.4982E-08	2.7984E+03	1.2357E+04	7.4300E+03	7.9286E+03	4.7130E-08
		Min	5.8109E+04	5.25341E+04	3.00391E+02	1.5215E+05	1.78791E+04	**3.0000E+02**	8.1618E+04	4.9904E+04	6.4370E+04	5.4896E+04	**3.0000E+02**
	50	Avg	2.1589E+05	1.54228E+05	3.00772E+02	3.4524E+05	8.59432E+04	3.0035E+02	2.8121E+05	2.0134E+05	1.7605E+05	1.6869E+05	3.0080E+02
		SD	2.6005E+04	1.46509E+04	4.49700E-01	5.0824E+04	1.15653E+04	1.1202E+00	1.2274E+05	1.9242E+04	2.4049E+04	2.1422E+04	1.8770E+00
		Min	1.4136E+05	1.17206E+05	3.00159E+02	2.7029E+05	6.34188E+04	**3.0000E+02**	1.8432E+05	1.5880E+05	1.4855E+05	1.4097E+05	**3.0000E+02**
	100	Avg	5.5899E+05	4.90388E+05	3.03809E+02	1.0158E+06	3.38128E+05	1.2652E+04	5.2875E+05	5.5477E+05	3.3529E+05	3.2481E+05	3.0380E+02
		SD	4.0284E+04	2.81876E+04	2.24693E+00	1.4440E+05	3.26822E+04	4.7457E+03	6.9785E+05	3.5187E+04	1.5851E+04	1.6648E+04	2.2470E+00
		Min	4.4578E+05	4.33909E+05	3.00802E+02	5.9410E+05	2.86574E+05	7.8656E+03	3.4532E+05	4.6124E+05	2.8379E+05	2.8274E+05	**3.0080E+02**
F_4	30	Avg	8.7962E+03	4.74768E+02	4.60272E+02	2.6637E+03	4.54630E+02	4.8515E+02	1.7818E+04	6.6414E+02	4.5383E+03	8.6132E+03	4.0700E+02
		SD	2.4023E+03	8.39620E-01	1.38574E+00	6.6116E+02	2.11234E+01	2.1747E+01	2.2449E+03	2.4966E+01	1.7472E+03	3.0115E+03	2.0130E+01
		Min	9.5796E+02	4.72957E+02	4.59145E+02	1.7997E+03	4.00623E+02	4.2667E+02	1.3681E+04	6.2123E+02	1.6121E+03	2.4834E+03	**4.0000E+02**
	50	Avg	3.2203E+04	4.97679E+02	4.32383E+02	2.0362E+04	4.86490E+02	5.5273E+02	3.7420E+04	1.1372E+03	1.5123E+04	2.4220E+04	4.6010E+02
		SD	8.0518E+03	9.11201E-01	1.40903E+01	4.1548E+03	5.39561E+01	3.5298E+01	3.4866E+03	7.9705E+01	4.7158E+03	4.0857E+03	3.5280E+01
		Min	1.9420E+03	4.95839E+02	4.28553E+02	1.4662E+04	4.19149E+02	4.9726E+02	2.9372E+04	9.8398E+02	8.1262E+03	1.5676E+04	**4.0010E+02**
	100	Avg	1.1900E+05	6.21373E+02	6.05697E+02	7.7024E+04	6.09167E+02	6.8798E+02	1.0554E+05	2.8265E+03	4.3815E+04	6.9631E+04	5.7670E+02
		SD	1.2735E+04	2.04354E+01	1.23057E+01	1.8604E+04	2.74908E+01	4.9410E+01	9.1309E+03	2.0743E+02	6.5825E+03	9.2090E+03	3.9180E+01
		Min	8.7791E+04	5.59811E+02	5.97357E+02	4.6944E+04	5.29741E+02	5.9895E+02	8.1504E+04	2.3022E+03	3.0973E+04	5.1544E+04	**5.0480E+02**
F_5	30	Avg	8.8658E+02	5.82814E+02	6.23725E+02	8.6937E+02	6.28983E+02	6.0667E+02	9.5529E+02	6.6639E+02	8.7466E+02	7.9841E+02	6.0510E+02
		SD	1.7864E+01	8.90438E+00	9.08148E+00	2.5356E+01	8.67157E+00	3.4586E+01	2.2592E+01	1.1275E+01	5.3659E+01	3.2172E+01	2.7520E+01
		Min	8.4156E+02	5.64532E+02	6.08022E+02	8.3413E+02	6.07340E+02	5.6970E+02	8.8793E+02	6.4082E+02	7.6870E+02	7.4093E+02	**5.6170E+02**
	50	Avg	1.3057E+03	6.78840E+02	7.97185E+02	1.2054E+03	7.84647E+02	7.7860E+02	1.2279E+03	8.6183E+02	1.1285E+03	1.0717E+03	6.7880E+02
		SD	8.6888E+01	1.07869E+01	1.07193E+01	5.7217E+01	1.24118E+01	6.6596E+01	1.6631E+01	2.7229E+01	3.8917E+01	3.7360E+01	1.0790E+01
		Min	9.2568E+02	**6.53673E+02**	7.67848E+02	1.0904E+03	7.55679E+02	6.9302E+02	1.1950E+03	7.7358E+02	1.0452E+03	1.0049E+03	6.5370E+02
	100	Avg	2.4641E+03	9.77358E+02	1.22908E+03	2.2214E+03	1.25535E+03	1.2515E+03	2.1535E+03	1.5050E+03	1.9735E+03	1.9342E+03	9.89907E+02
		SD	6.1847E+01	2.21133E+01	2.48664E+01	8.0875E+01	2.25969E+01	1.2760E+02	2.5318E+01	4.1603E+01	7.3372E+01	5.2973E+01	6.39795E+01
		Min	2.2319E+03	9.27454E+02	1.17684E+03	2.1096E+03	1.22091E+03	9.8952E+02	2.1078E+03	1.3954E+03	1.7790E+03	1.8151E+03	**8.74103E+02**
F_6	30	Avg	6.8024E+02	6.00000E+02	6.00007E+02	6.6912E+02	6.00000E+02	6.3388E+02	6.9909E+02	6.2271E+02	6.8207E+02	6.6464E+02	6.0040E+02
		SD	7.1173E+00	2.82486E-08	7.70335E-04	7.4442E+00	5.70562E-06	1.2043E+01	5.8258E+00	1.9290E+00	1.2282E+01	8.1810E+00	3.1930E-01
		Min	6.6292E+02	**6.00000E+02**	6.00005E+02	6.5449E+02	**6.00000E+02**	6.1872E+02	6.8315E+02	6.1665E+02	6.5565E+02	6.4427E+02	**6.0000E+02**
	50	Avg	7.0339E+02	6.00000E+02	6.00028E+02	6.9189E+02	6.00000E+02	6.4664E+02	7.1328E+02	6.3189E+02	6.9623E+02	6.8197E+02	6.0200E+02
		SD	4.2812E+00	1.51280E-06	4.61072E-03	8.9940E+00	1.46675E-04	1.1677E+01	3.6064E+00	1.6688E+00	3.5215E+00	5.2511E+00	9.6060E-01
		Min	6.9014E+02	**6.00000E+02**	6.00019E+02	6.7741E+02	**6.00000E+02**	6.2956E+02	7.0121E+02	6.2834E+02	6.8697E+02	6.7199E+02	**6.0000E+02**
	100	Avg	7.2059E+02	6.00001E+02	6.00002E+02	7.1524E+02	6.00001E+02	6.5828E+02	7.1716E+02	6.4507E+02	7.0331E+02	7.0080E+02	6.0810E+02
		SD	1.7537E+01	1.30006E-04	4.90414E-04	9.2902E+00	2.21072E-04	5.7566E+00	2.0336E+00	1.7721E+00	4.0297E+00	3.9222E+00	1.9810E+00
		Min	6.3752E+02	6.00001E+02	6.00001E+02	7.0349E+02	**6.00000E+02**	6.4785E+02	7.1387E+02	6.4167E+02	6.9384E+02	6.8922E+02	**6.0000E+02**
F_7	30	Avg	2.1737E+03	8.25686E+02	8.69854E+02	1.2732E+03	8.70538E+02	8.6463E+02	1.4405E+03	1.0442E+03	1.3791E+03	1.3046E+03	8.2890E+02
		SD	1.1874E+02	5.94137E+00	1.02771E+01	4.1948E+01	1.23804E+01	4.8583E+01	3.2897E+01	3.4589E+01	6.8148E+01	5.9606E+01	2.9150E+01
		Min	1.9233E+03	8.16415E+02	8.45959E+02	1.2085E+03	8.39825E+02	8.1999E+02	1.3832E+03	9.5780E+02	1.2097E+03	1.1810E+03	**7.7140E+02**
	50	Avg	3.8880E+03	9.54593E+02	1.06477E+03	2.0218E+03	1.05434E+03	1.0107E+03	2.0741E+03	1.4962E+03	1.9645E+03	1.8639E+03	1.0560E+03
		SD	1.9459E+02	1.32965E+01	1.29841E+01	1.4399E+02	1.76118E+01	4.5724E+01	3.4471E+01	3.9981E+01	8.3372E+01	4.9887E+01	6.5600E+01
		Min	3.4431E+03	9.29913E+02	1.03439E+03	1.7427E+03	1.01700E+03	9.4905E+02	2.0062E+03	1.4147E+03	1.7965E+03	1.7449E+03	**9.2510E+02**
	100	Avg	9.2300E+03	1.36617E+03	1.55382E+03	3.8176E+03	1.60130E+03	1.5681E+03	4.0494E+03	3.0703E+03	3.8736E+03	3.7491E+03	2.3720E+03
		SD	3.8246E+02	3.91775E+01	2.38208E+01	1.6321E+02	3.21338E+01	1.3059E+02	5.5783E+01	1.2351E+02	1.0088E+02	6.2638E+01	2.9310E+02
		Min	8.2672E+03	**1.29650E+03**	1.48682E+03	3.5312E+03	1.51088E+03	1.3476E+03	3.8862E+03	2.8598E+03	3.5734E+03	3.5938E+03	1.6940E+03
F_8	30	Avg	1.2005E+03	8.83762E+02	9.26352E+02	1.1250E+03	9.27306E+02	9.1412E+02	1.1774E+03	9.5941E+02	1.0816E+03	1.0264E+03	8.9350E+02
		SD	5.1546E+01	6.78663E+00	6.87944E+00	1.9217E+01	1.34635E+01	2.3840E+01	1.5620E+01	1.4659E+01	3.3080E+01	2.9485E+01	2.7460E+01
		Min	9.8322E+02	8.69400E+02	9.12647E+02	1.0875E+03	9.01012E+02	8.7363E+02	1.1443E+03	9.2285E+02	9.9731E+02	9.7469E+02	**8.4970E+02**
	50	Avg	1.5875E+03	9.74029E+02	1.09424E+03	1.5594E+03	1.08191E+03	1.0548E+03	1.5555E+03	1.1551E+03	1.4219E+03	1.4194E+03	9.7400E+02
		SD	1.3539E+02	1.01725E+01	1.31150E+01	5.5989E+01	1.19607E+01	6.7622E+01	2.2897E+01	2.1828E+01	4.6185E+01	4.2242E+01	1.0170E+01
		Min	1.1247E+03	9.52334E+02	1.05400E+03	1.4823E+03	1.05861E+03	9.5621E+02	1.4958E+03	1.0973E+03	1.3108E+03	1.3407E+03	**9.5230E+02**
	100	Avg	2.8533E+03	1.26052E+03	1.52924E+03	2.6666E+03	1.56536E+03	1.5201E+03	2.6500E+03	1.8065E+03	2.4568E+03	2.4094E+03	1.2610E+03
		SD	5.0121E+01	1.98577E+01	2.15518E+01	1.2315E+02	2.47552E+01	1.2043E+02	2.3686E+01	4.1523E+01	7.0714E+01	7.6111E+01	1.9860E+01
		Min	2.7606E+03	1.21801E+03	1.48909E+03	2.5217E+03	1.50451E+03	1.3549E+03	2.6037E+03	1.7178E+03	2.3244E+03	2.2409E+03	**1.21800E+03**
F_9	30	Avg	1.6405E+04	9.00000E+02	9.01822E+02	1.3481E+04	9.00000E+02	4.1709E+03	1.3072E+04	4.6833E+03	8.7082E+03	5.5521E+03	1.1770E+03
		SD	1.7333E+03	5.20698E-09	7.43058E-01	2.1227E+03	8.66746E-13	1.9490E+03	1.0923E+03	5.6890E+02	1.7165E+03	7.9506E+02	4.9130E+02
		Min	1.3021E+04	**9.00000E+02**	9.00610E+02	9.9785E+03	**9.00000E+02**	1.0006E+03	1.0976E+04	3.7851E+03	4.2391E+03	4.0883E+03	9.1280E+02
	50	Avg	4.6209E+04	9.00065E+02	9.00601E+02	4.0622E+04	9.00040E+02	1.0472E+04	4.3812E+04	1.4997E+04	3.2006E+04	2.1715E+04	3.2650E+03
		SD	8.4768E+03	8.60611E-02	2.86121E-01	7.8803E+03	9.46880E-02	3.5029E+03	1.7381E+03	1.8109E+03	4.7760E+03	2.6341E+03	1.2580E+03
		Min	9.0094E+03	9.00003E+02	9.00117E+02	2.9135E+04	**9.00000E+02**	3.8562E+03	3.9073E+04	1.0917E+04	2.0792E+04	1.6922E+04	1.3720E+03
	100	Avg	1.3144E+05	1.27444E+03	9.00001E+02	1.0702E+05	9.01834E+02	2.3192E+04	8.7631E+04	5.1289E+04	6.3032E+04	5.5916E+04	9.0000E+02
		SD	7.5124E+03	7.73202E+01	1.13537E-03	8.6919E+03	1.95290E+00	2.6925E+03	3.2482E+03	3.7619E+03	4.2155E+03	5.0778E+03	1.1350E-03
		Min	1.1015E+05	1.14390E+03	**9.00000E+02**	9.2144E+04	9.00090E+02	1.7090E+04	8.0800E+04	4.2854E+04	5.7250E+04	4.4095E+04	**9.0000E+02**
F_{10}	30	Avg	8.1157E+03	4.70567E+03	5.66929E+03	8.1117E+03	6.10576E+03	4.7881E+03	9.2130E+03	4.9636E+03	7.8327E+03	6.5839E+03	3.3750E+03
		SD	2.4935E+02	2.11542E+02	3.20365E+02	3.1526E+02	2.30270E+02	5.9682E+02	2.8290E+02	2.5851E+02	5.8524E+02	4.9526E+02	6.1790E+02
		Min	7.5312E+03	4.29487E+03	4.63041E+03	7.1855E+03	5.65151E+03	3.6607E+03	8.6102E+03	4.3198E+03	6.3170E+03	5.4880E+03	**2.0670E+03**
	50	Avg	1.4383E+04	8.34560E+03	1.07290E+04	1.4727E+04	1.09306E+04	7.6818E+03	1.5944E+04	8.5586E+03	1.3516E+04	1.2136E+04	6.3560E+03
		SD	4.6349E+02	3.94629E+02	3.44535E+02	2.3280E+02	3.90368E+02	1.1831E+03	5.1500E+02	3.2754E+02	7.6239E+02	7.0069E+02	7.8150E+02
		Min	1.3104E+04	7.63074E+03	9.95302E+03	1.4309E+04	9.91393E+03	5.6360E+03	1.4747E+04	7.9418E+03	1.2133E+04	1.0864E+04	**4.4670E+03**
	100	Avg	3.0736E+04	1.89002E+04	2.68139E+04	3.1673E+04	2.54144E+04	1.4859E+04	3.3432E+04	1.9455E+04	2.9798E+04	2.7769E+04	1.4680E+04
		SD	2.1694E+03	8.46416E+02	3.94468E+02	5.3225E+02	5.76029E+02	1.0340E+03	6.9638E+02	4.7398E+02	1.4684E+03	1.1675E+03	1.2160E+03
		Min	2.0573E+04	1.77717E+04	2.58708E+04	3.0751E+04	2.38409E+04	1.3103E+04	3.1718E+04	1.7891E+04	2.6870E+04	2.4907E+04	**1.2580E+04**
Ranking	**30**	**W|T|L**	0|0|9	0|2|7	0|0|9	0|0|9	0|2|7	0|1|8	0|0|9	0|0|9	0|0|9	0|0|9	**6|2|1**
	50	**W|T|L**	0|0|9	1|1|7	0|0|9	0|0|9	1|1|7	0|1|8	0|0|9	0|0|9	0|0|9	0|0|9	**5|2|2**
	100	**W|T|L**	0|0|9	1|0|8	0|1|8	0|0|9	0|1|8	0|0|9	0|0|9	0|0|9	0|0|9	0|0|9	**7|1|1**

Table 3 Comparison of optimization results obtained from hybrid test functions.

Func.	D	Metrics	jDE (2006)	DE/BBO (2010)	CoDE (2011)	Jaya (2016)	MKE (2016)	SSA (2017)	EEGWO (2018)	WDE (2018)	MWOA (2018)	AOA (2021)	QANA
F_{11}	30	Avg	9.4348E+03	1.1790E+03	1.16488E+03	1.7504E+04	1.16579E+03	1.2842E+03	9.6669E+03	1.4077E+03	5.6278E+03	3.3556E+03	1.1790E+03
		SD	2.3386E+03	6.3989E+00	7.43028E+00	4.6855E+03	2.89988E+01	4.6494E+01	2.0140E+03	3.5383E+01	2.1293E+03	1.5184E+03	3.4750E+01
		Min	3.6150E+03	1.1671E+03	1.14927E+03	9.3021E+03	1.13380E+03	1.1994E+03	6.3148E+03	1.3323E+03	2.6524E+03	1.7261E+03	**1.1250E+03**
	50	Avg	2.1877E+04	1.4074E+03	1.21476E+03	3.7048E+04	1.24487E+03	1.3975E+03	2.4354E+04	2.2099E+03	1.1582E+04	1.3950E+04	1.2760E+03
		SD	3.9172E+03	2.3622E+01	7.27766E+00	1.2352E+04	2.30910E+01	4.8526E+01	2.1967E+03	1.7394E+02	3.3255E+03	3.4901E+03	4.7090E+01
		Min	1.4524E+04	1.3655E+03	1.20327E+03	2.2037E+04	1.20932E+03	1.2379E+03	1.8444E+04	1.9491E+03	5.3654E+03	7.2569E+03	**1.1510E+03**
	100	Avg	2.1424E+05	2.4618E+03	1.36606E+03	3.4426E+05	1.79281E+03	2.5689E+03	6.4587E+05	3.1955E+04	1.6947E+05	1.5678E+05	1.3660E+03
		SD	2.5545E+04	1.2358E+02	6.40393E+01	7.9505E+04	4.99390E+01	2.0880E+02	4.5986E+05	5.7921E+03	3.6803E+04	2.2761E+04	6.4040E+01
		Min	1.6327E+05	2.2309E+03	1.24704E+03	2.3856E+05	1.67878E+03	2.0232E+03	2.1688E+05	1.8192E+04	9.7258E+04	1.1691E+05	**1.24700E+03**
F_{12}	30	Avg	1.0423E+10	4.6767E+05	3.33261E+03	2.2463E+09	4.96378E+04	3.7310E+06	1.4816E+10	2.5752E+07	2.6407E+09	6.7672E+09	3.3180E+03
		SD	1.8699E+09	1.6981E+05	2.73117E+02	7.3208E+08	2.93083E+04	2.5583E+06	1.9592E+09	6.7742E+06	1.3133E+09	1.7547E+09	1.9160E+03
		Min	6.0852E+09	2.4952E+05	2.79546E+03	1.4570E+09	6.98602E+03	6.5758E+05	1.0698E+10	1.1517E+07	6.7688E+08	3.4529E+09	**2.0780E+03**
	50	Avg	4.4341E+10	1.3455E+06	8.76528E+03	2.6299E+10	2.09526E+05	1.8651E+07	8.7310E+10	2.5033E+08	2.0616E+10	5.5215E+10	4.2320E+03
		SD	8.0361E+09	3.7206E+05	4.01566E+03	8.5272E+09	2.07857E+05	1.3538E+07	7.7120E+09	6.2257E+07	1.1721E+10	9.9616E+09	4.6780E+02
		Min	3.2447E+10	5.8661E+05	5.25574E+03	1.3093E+10	3.48460E+04	2.3044E+06	7.2363E+10	1.4234E+08	7.1153E+09	2.5806E+10	**3.2410E+03**
	100	Avg	1.7331E+11	1.2555E+06	3.40009E+05	1.1263E+11	1.23864E+06	7.1194E+07	2.0553E+11	1.8388E+09	7.9744E+10	1.7028E+11	1.2040E+04
		SD	1.3246E+10	3.2393E+05	1.61495E+05	1.9487E+10	4.89616E+05	2.5354E+07	1.0774E+10	2.6162E+08	1.9011E+10	2.1475E+10	5.0820E+03
		Min	1.2966E+11	8.1019E+05	1.61818E+05	8.4069E+10	6.34381E+05	2.3311E+07	1.8619E+11	1.2222E+09	4.4149E+10	1.2672E+11	**4.5820E+03**
F_{13}	30	Avg	1.6215E+09	1.3711E+03	1.39430E+03	2.3123E+08	1.45806E+03	1.5189E+05	1.4209E+10	3.5166E+05	2.4580E+08	4.3645E+04	1.3750E+03
		SD	4.7617E+08	5.4800E+00	6.55020E+00	1.7703E+08	3.24120E+01	1.0123E+05	3.8299E+09	1.4384E+05	2.4321E+08	4.0071E+04	4.0160E+01
		Min	3.2672E+08	1.3610E+03	1.38318E+03	3.8914E+07	1.40969E+03	1.5811E+04	4.1000E+09	1.1923E+05	4.5192E+06	1.9704E+04	**1.3160E+03**
	50	Avg	1.4619E+10	1.2415E+05	1.51544E+03	1.1043E+10	2.43031E+03	1.0759E+05	4.9109E+10	3.9312E+06	3.8725E+09	3.4778E+09	5.4030E+03
		SD	4.5740E+09	6.0585E+04	2.51748E+01	2.2062E+09	1.37405E+03	4.7200E+04	9.0470E+09	1.3328E+06	3.0887E+09	3.4837E+09	7.7010E+03
		Min	7.0465E+08	4.9200E+04	**1.44901E+03**	7.0309E+09	1.63933E+03	4.5776E+04	2.6054E+10	1.3272E+06	7.0930E+08	8.6005E+06	1.6000E+03
	100	Avg	3.4177E+10	6.5799E+04	1.83584E+03	1.7483E+10	7.16860E+03	7.3147E+04	4.7863E+10	1.6331E+07	1.0573E+10	3.3969E+10	1.1980E+04
		SD	8.4495E+09	2.0274E+04	1.22993E+02	3.8097E+09	5.18801E+03	4.4264E+04	4.0124E+09	3.4564E+06	4.2632E+09	3.7911E+09	7.5780E+03
		Min	6.2254E+08	4.8454E+04	1.68800E+03	9.2552E+09	1.68536E+03	3.0036E+04	4.1497E+10	1.1102E+07	3.7600E+09	2.6079E+10	**2.2860E+03**
F_{14}	30	Avg	7.8961E+05	2.2788E+03	1.45121E+03	1.1882E+06	1.46377E+03	1.0705E+04	7.4613E+06	2.5844E+03	1.1930E+06	4.8518E+04	1.4710E+03
		SD	4.1695E+05	4.8358E+02	3.34326E+00	6.5585E+05	5.31697E+00	6.6506E+03	4.7391E+06	3.5645E+02	1.0504E+06	3.6007E+04	2.1420E+01
		Min	1.5858E+05	1.7743E+03	1.44328E+03	2.6106E+05	1.45448E+03	1.7371E+03	1.3601E+06	2.0833E+03	4.6250E+03	2.8773E+03	**1.4380E+03**
	50	Avg	8.7847E+06	4.8618E+03	1.49663E+03	6.3919E+06	1.54733E+03	5.0162E+04	1.5906E+08	2.0782E+04	6.8215E+06	4.2734E+05	1.5360E+03
		SD	3.2772E+06	1.5136E+03	7.86784E+00	2.4324E+06	1.39052E+01	4.4212E+04	6.9400E+07	9.3857E+03	7.9215E+06	3.4595E+05	3.8270E+01
		Min	2.7715E+06	2.1487E+03	1.48080E+03	2.9556E+06	1.51920E+03	1.4094E+04	5.3397E+07	6.5861E+03	1.9417E+05	5.7380E+04	**1.4700E+03**
	100	Avg	7.0261E+07	3.1676E+04	1.53450E+03	8.9302E+07	4.16418E+03	3.5226E+05	1.5144E+08	3.8306E+05	2.3778E+07	1.9818E+07	1.5340E+03
		SD	1.6673E+07	1.3196E+04	6.53155E+01	2.8599E+07	5.53243E+03	1.9468E+05	5.6330E+07	1.1598E+05	9.2376E+06	1.1915E+07	6.5320E+01
		Min	4.1255E+07	1.4696E+04	1.45642E+03	4.9752E+07	1.90262E+03	1.1109E+05	5.5592E+07	1.3028E+05	9.3017E+06	4.7559E+06	**1.4560E+03**
F_{15}	30	Avg	1.5281E+08	2.0380E+03	1.53134E+03	6.6726E+07	1.55919E+03	8.5724E+04	6.2937E+08	1.1176E+04	3.4799E+07	2.4682E+04	1.5310E+03
		SD	6.6426E+07	1.7412E+02	4.27952E+00	4.4752E+07	2.06994E+01	7.7001E+04	2.5465E+08	3.6899E+03	6.4097E+07	1.0972E+04	4.2800E+00
		Min	3.4084E+07	1.6556E+03	**1.51671E+03**	6.4439E+06	1.54218E+03	1.4628E+04	2.6572E+08	5.7677E+03	9.3093E+04	1.4121E+04	1.5170E+03
	50	Avg	3.3704E+09	2.7581E+04	1.58464E+03	2.0027E+09	1.64778E+03	4.9401E+04	8.9693E+09	6.7629E+04	6.5295E+08	3.4265E+04	1.5850E+03
		SD	1.0385E+09	1.8434E+04	8.73875E+00	5.8348E+08	1.76004E+01	3.3124E+04	2.0669E+09	2.4471E+04	8.9929E+08	8.3451E+03	8.7390E+00
		Min	1.6816E+09	5.1402E+03	1.56326E+03	1.1316E+09	1.61059E+03	1.8034E+04	4.7018E+09	2.0594E+04	1.4485E+07	1.9974E+04	**1.5630E+03**
	100	Avg	1.2877E+10	8.1637E+03	1.69441E+03	1.2160E+10	4.99309E+03	7.5260E+04	2.6254E+10	5.0827E+05	3.8932E+09	5.6218E+09	1.6940E+03
		SD	3.4854E+09	5.0625E+03	5.01001E+01	1.8771E+09	2.62907E+03	2.9758E+04	2.5451E+09	1.8979E+05	2.0004E+09	2.2013E+09	5.0100E+01
		Min	9.7581E+07	1.6555E+03	**1.60300E+03**	8.9145E+09	1.94537E+03	2.0549E+04	2.1985E+10	9.8283E+04	6.4742E+08	1.6912E+09	**1.60300E+03**
F_{16}	30	Avg	4.1870E+03	2.1775E+03	2.10938E+03	4.4938E+03	2.24790E+03	2.5286E+03	6.6843E+03	2.3920E+03	4.1417E+03	3.6495E+03	2.3060E+03
		SD	3.1518E+02	1.0420E+02	9.21428E+01	3.3337E+02	1.96507E+02	3.3654E+02	8.3922E+02	1.1171E+02	5.8147E+02	4.4912E+02	2.6430E+02
		Min	3.3538E+03	1.9910E+03	1.94218E+03	3.7945E+03	1.87071E+03	2.0093E+03	4.8220E+03	2.1131E+03	3.2794E+03	2.8626E+03	**1.7760E+03**
	50	Avg	7.2903E+03	2.9696E+03	2.95177E+03	7.3305E+03	3.20908E+03	3.2215E+03	1.0953E+04	3.2216E+03	6.4785E+03	5.6450E+03	3.1980E+03
		SD	3.4458E+02	1.1168E+02	1.83654E+02	3.9374E+02	3.37159E+02	3.5623E+02	8.0149E+02	1.5245E+02	8.9048E+02	1.0956E+03	3.5040E+02
		Min	6.3167E+03	2.7805E+03	2.41128E+03	6.7923E+03	**2.30421E+03**	2.6558E+03	9.6273E+03	2.8707E+03	4.9417E+03	3.5804E+03	2.5380E+03
	100	Avg	1.8285E+04	5.6988E+03	6.99216E+03	1.5666E+04	7.06958E+03	5.8788E+03	2.4808E+04	6.3287E+03	1.6628E+04	1.7011E+04	7.0700E+03
		SD	1.1062E+03	4.4075E+02	4.22176E+02	1.0350E+03	7.31138E+02	8.8382E+02	1.8634E+03	3.3996E+02	2.4771E+03	2.5105E+03	7.3110E+02
		Min	1.5531E+04	4.3999E+03	5.74653E+03	1.3950E+04	4.30614E+03	3.9403E+03	2.0705E+04	5.5594E+03	1.2823E+04	1.3005E+04	**4.3060E+03**
F_{17}	30	Avg	3.0753E+03	1.8960E+03	1.82996E+03	2.9659E+03	1.82828E+03	2.0374E+03	5.3238E+03	1.8976E+03	2.7179E+03	2.5859E+03	1.8280E+03
		SD	1.6658E+02	2.5350E+01	1.56029E+01	1.6025E+02	7.24457E+01	1.4527E+02	1.4125E+03	3.4890E+01	2.2578E+02	3.0824E+02	7.2450E+01
		Min	2.5450E+03	1.8408E+03	1.80427E+03	2.7188E+03	1.76080E+03	1.7923E+03	3.7253E+03	1.8388E+03	2.3845E+03	2.0400E+03	**1.7610E+03**
	50	Avg	6.6265E+03	2.3026E+03	2.59917E+03	5.5479E+03	2.73956E+03	2.9819E+03	1.1370E+04	2.7446E+03	5.0293E+03	4.0778E+03	2.3030E+03
		SD	7.9679E+02	1.0835E+02	1.15142E+02	3.8334E+02	2.21347E+02	3.3053E+02	4.4377E+03	1.0223E+02	9.9919E+02	4.1105E+02	1.0840E+02
		Min	4.4755E+03	2.1081E+03	2.36143E+03	5.0664E+03	2.28590E+03	2.4265E+03	6.2195E+03	2.4187E+03	3.8936E+03	3.4068E+03	**2.1080E+03**
	100	Avg	5.1415E+05	3.9499E+03	4.83190E+03	7.6073E+05	5.34097E+03	5.2044E+03	1.2144E+07	4.8938E+03	2.0036E+05	1.7268E+05	3.9500E+03
		SD	3.1338E+05	2.3470E+02	2.08411E+02	5.7562E+05	2.36691E+02	6.0949E+02	3.9465E+06	2.1438E+02	2.7182E+05	3.6699E+05	2.3470E+02
		Min	1.1359E+05	3.6052E+03	4.45812E+03	1.2364E+05	4.88443E+03	4.2869E+03	4.3295E+06	4.3503E+03	1.1105E+04	1.5551E+04	**3.6050E+03**
F_{18}	30	Avg	4.1540E+06	2.3497E+05	1.83792E+03	1.4565E+07	1.89735E+03	2.2251E+05	7.4325E+07	6.3816E+04	1.2185E+07	1.0342E+06	5.4430E+03
		SD	1.7236E+06	8.2168E+04	3.02465E+00	9.3462E+06	2.72327E+01	1.9426E+05	3.6071E+07	2.1796E+04	1.6410E+07	9.9731E+05	4.8860E+03
		Min	1.3147E+06	8.1183E+04	1.83300E+03	1.6083E+06	**1.87501E+03**	5.8523E+04	2.8515E+07	1.9633E+04	6.6014E+05	7.7898E+04	2.0580E+03
	50	Avg	5.3895E+07	1.3441E+06	1.85654E+03	4.6116E+07	4.77653E+03	4.6751E+05	2.3010E+08	3.8271E+05	5.4263E+07	1.9624E+07	3.2550E+04
		SD	1.5289E+07	4.4034E+05	4.98138E+00	1.7246E+07	2.88738E+03	2.9474E+05	7.9089E+07	1.3565E+05	4.2914E+07	1.6971E+07	2.3530E+04
		Min	3.1830E+07	4.8168E+05	**1.84792E+03**	1.4740E+07	2.27524E+03	1.6869E+05	6.6396E+07	1.9804E+05	2.3227E+06	3.1974E+06	5.7230E+03
	100	Avg	1.1412E+08	8.1554E+06	2.20826E+03	9.8762E+07	1.96014E+05	5.8366E+05	2.8541E+08	1.3593E+06	2.3938E+07	3.5921E+07	2.0050E+05
		SD	2.4781E+07	1.8663E+06	1.26999E+02	2.7891E+07	1.28321E+05	2.6377E+05	7.0735E+07	3.3247E+05	1.2670E+07	3.1432E+07	1.3060E+05
		Min	5.7100E+07	5.1896E+06	**2.01905E+03**	4.2476E+07	4.41351E+04	2.4130E+05	1.5080E+08	7.9803E+05	7.1403E+06	4.5043E+06	5.5080E+04
F_{19}	30	Avg	1.2483E+08	3.1195E+03	1.92406E+03	1.4510E+08	1.92920E+03	5.3397E+05	9.8692E+08	1.6543E+04	4.5161E+07	1.0930E+06	1.9710E+03
		SD	5.2753E+07	1.4974E+03	1.43646E+00	6.2577E+07	2.69165E+00	2.1373E+05	3.8598E+08	6.2127E+03	5.3009E+07	7.8987E+04	1.2930E+02
		Min	2.9403E+07	1.9281E+03	1.92153E+03	7.3932E+07	1.92321E+03	3.0256E+05	3.9580E+08	5.6089E+03	4.6419E+05	9.1318E+05	**1.9120E+03**
	50	Avg	1.5360E+09	4.1460E+03	1.94832E+03	4.1777E+08	1.97335E+03	1.0354E+06	5.0770E+09	4.8040E+04	2.2668E+08	4.6394E+05	1.9480E+03
		SD	3.3431E+08	1.7583E+03	4.02553E+00	2.3078E+08	7.55549E+00	5.2069E+05	1.0359E+09	1.8299E+04	3.2224E+08	1.2158E+04	4.0260E+00
		Min	9.6039E+08	2.0745E+03	**1.93770E+03**	1.0437E+08	1.95698E+03	1.6552E+05	3.5235E+09	1.9201E+04	6.5061E+06	4.4801E+05	1.9380E+03
	100	Avg	1.3307E+10	3.2785E+03	2.00146E+03	1.1479E+10	7.08199E+03	3.0299E+06	2.4107E+10	9.9814E+05	4.0596E+09	3.9262E+09	4.8910E+03
		SD	3.6241E+09	9.8395E+02	2.97843E+01	2.5247E+09	6.19023E+03	7.8694E+05	2.8436E+09	2.7978E+05	2.2019E+09	1.8397E+09	3.0180E+03
		Min	2.8715E+08	**2.0458E+03**	1.94955E+03	6.6328E+09	2.05124E+03	1.7296E+06	1.7954E+10	5.3588E+05	1.0269E+09	1.0837E+09	2.1990E+03
F_{20}	30	Avg	2.8279E+03	2.2053E+03	2.11700E+03	2.8180E+03	2.12255E+03	2.3926E+03	3.2902E+03	2.2245E+03	2.8095E+03	2.6882E+03	2.2300E+03
		SD	7.6261E+01	2.2649E+01	2.22305E+01	1.0958E+02	8.78013E+01	1.4434E+02	1.5977E+02	5.7903E+01	2.0747E+02	1.6742E+02	1.1350E+02
		Min	2.6681E+03	2.1699E+03	2.06657E+03	2.6316E+03	**2.02991E+03**	2.1675E+03	2.8488E+03	2.1174E+03	2.3463E+03	2.3289E+03	2.0440E+03
	50	Avg	3.9776E+03	2.5297E+03	2.59668E+03	4.2393E+03	2.82762E+03	3.0200E+03	4.6177E+03	2.7001E+03	3.8865E+03	3.4094E+03	2.5300E+03
		SD	1.9881E+02	8.5937E+01	9.94362E+01	1.7147E+02	1.54422E+02	2.2238E+02	1.2595E+02	9.6569E+01	3.7391E+02	2.2438E+02	8.5940E+01
		Min	3.3793E+03	2.3488E+03	2.42651E+03	3.8760E+03	2.62814E+03	2.7122E+03	4.4363E+03	2.5119E+03	3.1833E+03	2.9463E+03	**2.3490E+03**
	100	Avg	7.3307E+03	3.8052E+03	4.58539E+03	7.6776E+03	5.28051E+03	5.1172E+03	8.4479E+03	4.4884E+03	6.8020E+03	5.9404E+03	3.8050E+03
		SD	2.5886E+02	2.0804E+02	2.90978E+02	2.4990E+02	2.95067E+02	5.7195E+02	2.6272E+02	2.1884E+02	4.8984E+02	5.5229E+02	2.0800E+02
		Min	6.6453E+03	3.3111E+03	4.01515E+03	7.1310E+03	4.38207E+03	4.0519E+03	7.8082E+03	3.9664E+03	5.8230E+03	4.7573E+03	**3.3110E+03**
Ranking	**30**	**W|T|L**	0|0|10	0|0|10	1|0|9	0|0|10	2|0|8	0|0|10	0|0|10	0|0|10	0|0|10	0|0|10	**7|0|3**
	50	**W|T|L**	0|0|10	0|0|10	3|0|7	0|0|10	1|0|9	0|0|10	0|0|10	0|0|10	0|0|10	0|0|10	**6|0|4**
	100	**W|T|L**	0|0|10	1|0|9	2|0|8	0|0|10	0|0|10	0|0|10	0|0|10	0|0|10	0|0|10	0|0|10	**7|1|2**

Table 4 Comparison of optimization results obtained from composition test functions.

Func.	D	Metrics	jDE (2006)	DE/BBO (2010)	CoDE (2011)	Jaya (2016)	MKE (2016)	SSA (2017)	EEGWO (2018)	WDE (2018)	MWOA (2018)	AOA (2021)	QANA
F_{21}	30	Avg	2.2671E+03	2.1764E+03	2.42692E+03	2.6289E+03	2.43206E+03	2.3983E+03	2.8005E+03	2.4169E+03	2.6343E+03	2.5674E+03	2.1652E+03
		SD	1.3146E+00	8.7488E-01	9.00677E+00	2.7511E+01	9.41015E+00	5.3245E+01	3.0386E+01	6.1407E+01	4.5500E+01	5.0854E+01	2.6420E+01
		Min	2.2643E+03	2.1758E+03	2.40625E+03	2.5568E+03	2.42049E+03	2.2015E+03	2.7294E+03	2.2857E+03	2.5458E+03	2.4184E+03	**2.1033E+03**
	50	Avg	3.1340E+03	2.2232E+03	2.59940E+03	3.0208E+03	2.58467E+03	2.5611E+03	3.3073E+03	2.6530E+03	3.0278E+03	2.9872E+03	2.1833E+03
		SD	3.4887E+01	1.2353E+01	1.28400E+01	4.7368E+01	1.55329E+01	5.6519E+01	5.9658E+01	2.0569E+01	8.0556E+01	6.4315E+01	3.9369E+01
		Min	3.0544E+03	2.2185E+03	2.57759E+03	2.9007E+03	2.54671E+03	2.4802E+03	3.1583E+03	2.6125E+03	2.8329E+03	2.8701E+03	**2.1004E+03**
	100	Avg	4.4701E+03	2.2500E+03	3.05810E+03	4.0903E+03	3.08173E+03	3.0079E+03	5.1688E+03	3.3508E+03	4.4098E+03	4.5126E+03	2.2500E+03
		SD	3.6735E+02	2.4519E-09	4.64146E+01	9.7466E+01	3.83682E+01	1.3163E+02	1.4144E+02	3.9579E+01	1.4171E+02	1.7980E+02	0.0000E+00
		Min	2.9909E+03	**2.2500E+03**	2.86972E+03	3.9272E+03	3.00947E+03	2.8129E+03	4.8715E+03	3.2622E+03	4.1058E+03	4.2292E+03	**2.2500E+03**
F_{22}	30	Avg	2.3656E+03	2.2812E+03	2.30000E+03	9.4840E+03	3.57372E+03	3.3331E+03	9.7756E+03	2.7924E+03	8.2966E+03	7.8442E+03	2.3073E+03
		SD	3.4194E+00	5.4922E+00	3.13541E-05	5.9517E+02	2.31816E+03	1.8908E+03	4.7943E+02	9.3631E+01	1.4986E+03	9.4558E+02	3.0068E+01
		Min	2.3525E+03	2.2685E+03	2.30000E+03	7.6220E+03	2.30000E+03	2.3000E+03	8.5680E+03	2.6176E+03	4.7298E+03	5.2984E+03	**2.2448E+03**
	50	Avg	1.6104E+04	2.3926E+03	1.05973E+04	1.5732E+04	1.26262E+04	9.1307E+03	1.8080E+04	9.2154E+03	1.5389E+04	1.4669E+04	2.5014E+03
		SD	3.1831E+02	1.1739E+01	4.24287E+03	4.2421E+02	3.66704E+02	8.0237E+02	5.6351E+02	2.0333E+03	7.4551E+02	8.3866E+02	5.4068E+01
		Min	1.5311E+04	2.3715E+03	**2.30002E+03**	1.4410E+04	1.19492E+04	7.5498E+03	1.6542E+04	4.2257E+03	1.4013E+04	1.2398E+04	2.3960E+03
	100	Avg	3.3825E+04	2.3500E+03	2.76155E+04	3.3685E+04	2.74699E+04	1.8389E+04	3.6012E+04	2.1891E+04	3.2319E+04	3.1269E+04	2.3500E+03
		SD	5.1963E+02	3.0077E-11	5.30891E+03	2.7150E+02	6.78700E+02	1.4918E+03	5.7290E+02	5.5116E+02	1.1839E+03	1.1424E+03	0.0000E+00
		Min	3.2445E+04	**2.3500E+03**	2.30002E+03	3.3086E+04	2.59629E+04	1.6699E+04	3.4796E+04	2.0267E+04	2.9796E+04	2.9517E+04	**2.3500E+03**
F_{23}	30	Avg	4.6230E+03	2.8598E+03	2.76331E+03	3.2341E+03	2.77240E+03	2.7438E+03	3.7251E+03	2.7907E+03	3.1929E+03	3.3313E+03	2.5064E+03
		SD	1.7503E+02	7.0684E+00	6.61436E+00	5.1759E+01	9.69093E+00	2.2465E+01	1.2769E+02	3.3814E+01	1.1841E+02	1.1194E+02	1.6607E+01
		Min	4.0983E+03	2.8415E+03	2.75247E+03	3.1475E+03	2.74947E+03	2.7093E+03	3.5097E+03	2.7353E+03	2.9819E+03	3.1855E+03	**2.5000E+03**
	50	Avg	4.0610E+03	3.1761E+03	3.01872E+03	4.0999E+03	3.00858E+03	2.9611E+03	4.7796E+03	3.1251E+03	3.8989E+03	4.2211E+03	2.5000E+03
		SD	1.9767E+02	1.7394E+01	1.45514E+01	1.0809E+02	2.32928E+01	4.1628E+01	1.8555E+02	5.9089E+01	1.7389E+02	1.9954E+02	1.8501E-12
		Min	3.2563E+03	3.1384E+03	2.98302E+03	3.8832E+03	2.94650E+03	2.8923E+03	4.5066E+03	3.2970E+03	3.5617E+03	3.8457E+03	**2.5000E+03**
	100	Avg	6.0659E+03	3.8150E+03	3.52013E+03	5.4204E+03	3.46914E+03	3.4001E+03	7.7346E+03	3.6854E+03	5.7094E+03	6.5220E+03	3.1223E+03
		SD	2.1157E+02	3.3918E+01	2.36103E+01	1.4425E+02	2.86060E+01	9.3884E+01	4.0842E+02	4.1718E+01	2.8492E+02	4.3067E+02	1.9511E+01
		Min	5.6959E+03	3.7545E+03	3.44244E+03	5.1741E+03	3.40829E+03	3.2208E+03	7.0134E+03	3.5643E+03	5.1440E+03	5.8060E+03	**3.0941E+03**
F_{24}	30	Avg	4.8943E+03	3.2637E+03	2.94762E+03	3.3166E+03	2.95591E+03	2.9101E+03	4.0234E+03	3.0007E+03	3.3267E+03	3.6008E+03	2.6000E+03
		SD	1.5018E+02	2.4413E+02	9.80431E+00	5.3826E+01	1.15080E+01	2.5642E+01	2.0375E+02	4.6389E+01	9.8969E+01	1.5286E+02	0.0000E+00
		Min	4.5935E+03	2.7000E+03	2.92432E+03	3.2197E+03	2.93206E+03	2.8652E+03	3.6930E+03	2.7789E+03	3.1638E+03	3.2764E+03	**2.6000E+03**
	50	Avg	4.3865E+03	2.7000E+03	3.17236E+03	3.9891E+03	3.19200E+03	3.0861E+03	5.3847E+03	3.3654E+03	4.1366E+03	4.6878E+03	2.6000E+03
		SD	2.3228E+02	2.9377E-02	2.36329E+01	1.1089E+02	1.37591E+01	5.4093E+01	2.3452E+02	2.8369E+01	1.7559E+02	1.5495E+02	0.0000E+00
		Min	3.4027E+03	2.7000E+03	3.11399E+03	3.7777E+03	3.17363E+03	3.0071E+03	4.9770E+03	3.3205E+03	3.6965E+03	4.4176E+03	**2.6000E+03**
	100	Avg	9.2133E+03	5.1738E+03	3.96858E+03	8.0364E+03	4.02620E+03	3.8599E+03	1.2668E+04	4.4774E+03	7.6799E+03	1.0522E+04	3.6993E+03
		SD	1.0614E+03	2.6400E+02	4.65180E+01	3.6699E+02	2.76615E+01	9.2466E+01	1.0572E+03	5.1954E+01	6.8832E+02	8.2721E+02	5.3579E+01
		Min	4.5494E+03	4.1124E+03	3.87630E+03	7.2488E+03	3.96884E+03	3.7078E+03	9.5966E+03	4.3508E+03	6.5705E+03	9.2789E+03	**3.5609E+03**
F_{25}	30	Avg	7.6679E+03	2.9142E+03	2.88689E+03	3.5120E+03	2.88677E+03	2.8962E+03	5.5833E+03	3.0101E+03	3.7525E+03	4.3773E+03	2.7000E+03
		SD	8.2380E+02	4.6518E-01	2.12282E-02	1.3970E+02	3.54458E-02	1.8562E+01	4.4998E+02	2.1082E+01	2.1852E+02	4.9521E+02	0.0000E+00
		Min	6.6433E+03	2.9131E+03	2.88685E+03	3.2669E+03	2.88671E+03	2.8844E+03	4.3756E+03	2.9663E+03	3.4428E+03	3.5134E+03	**2.7000E+03**
	50	Avg	2.2685E+04	3.0040E+03	2.98029E+03	8.7708E+03	2.98992E+03	3.0410E+03	1.5254E+04	3.5154E+03	9.2572E+03	1.3817E+04	2.7000E+03
		SD	2.3801E+03	2.6606E+01	2.47206E-02	1.6277E+03	2.48998E+01	2.7719E+01	7.3820E+02	6.4439E+01	9.7083E+02	1.2774E+03	0.0000E+00
		Min	1.8286E+04	2.9801E+03	2.98025E+03	6.4974E+03	2.97736E+03	3.0016E+03	1.3783E+04	3.4042E+03	7.4031E+03	1.0826E+04	**2.7000E+03**
	100	Avg	6.1079E+04	3.2168E+03	3.23580E+03	2.5316E+04	3.23826E+03	3.3102E+03	2.8655E+04	5.4520E+03	1.6425E+04	2.2894E+04	3.2380E+03
		SD	5.2046E+03	1.8799E+01	3.66979E+01	5.1744E+03	6.02889E+01	5.6075E+01	1.4836E+03	1.6028E+02	1.2973E+03	1.6431E+03	6.0290E+01
		Min	4.5513E+04	3.1869E+03	3.13865E+03	1.7660E+04	3.13803E+03	3.1814E+03	2.5327E+04	5.1315E+03	1.3876E+04	1.8955E+04	**3.1380E+03**
F_{26}	30	Avg	1.0505E+04	5.1480E+03	4.61686E+03	9.9355E+03	4.80906E+03	4.3939E+03	1.1706E+04	3.9541E+03	8.6007E+03	9.2182E+03	2.8000E+03
		SD	1.1012E+03	7.8146E+01	5.23840E+02	7.3475E+02	1.03663E+02	8.4655E+02	4.0834E+02	1.3385E+02	9.9335E+02	8.8225E+02	0.0000E+00
		Min	7.2103E+03	4.9337E+03	2.90003E+03	8.6869E+03	4.56750E+03	**2.8000E+03**	1.0887E+04	3.6496E+03	6.9556E+03	7.1599E+03	**2.8000E+03**
	50	Avg	1.7789E+04	7.2460E+03	6.52022E+03	2.0108E+04	6.53359E+03	3.8242E+03	1.7697E+04	5.9092E+03	1.5394E+04	1.5977E+04	2.8000E+03
		SD	1.8008E+03	1.5682E+02	1.65140E+02	1.3910E+03	1.91082E+02	1.4798E+03	3.9809E+02	7.0889E+02	1.0653E+03	9.9457E+02	0.0000E+00
		Min	1.0665E+04	6.8244E+03	6.10094E+03	1.7408E+04	6.24954E+03	2.9000E+03	1.6968E+04	4.6609E+03	1.3317E+04	1.3901E+04	**2.8000E+03**
	100	Avg	5.3689E+04	1.4200E+04	1.20679E+04	6.0969E+04	1.31416E+04	1.0901E+04	5.6323E+04	1.7192E+04	4.3877E+04	4.9016E+04	1.0039E+04
		SD	2.8216E+03	2.9976E+02	7.81799E+02	6.1100E+03	3.76514E+02	3.7419E+03	1.9649E+03	1.7471E+03	3.1872E+03	2.8055E+03	7.6525E+02
		Min	4.6537E+04	1.3688E+04	9.96363E+03	5.3711E+04	1.21777E+04	**2.9000E+03**	5.2511E+04	1.1547E+04	3.6449E+04	4.2886E+04	8.8167E+03
F_{27}	30	Avg	5.6706E+03	3.4309E+03	3.20121E+03	3.4202E+03	3.19393E+03	3.2292E+03	4.9984E+03	3.2648E+03	3.6125E+03	4.0910E+03	2.9304E+03
		SD	1.5092E+02	3.3475E+00	5.13612E+00	5.3306E+01	1.26436E+01	1.4680E+01	3.2786E+02	6.0628E+00	1.3912E+02	2.3832E+02	7.1430E+01
		Min	5.2777E+03	3.4239E+03	3.18811E+03	3.3402E+03	3.16845E+03	3.2130E+03	4.3888E+03	3.2532E+03	3.3563E+03	3.6795E+03	**2.9000E+03**
	50	Avg	5.5440E+03	3.5389E+03	3.22054E+03	4.5516E+03	3.24440E+03	3.3406E+03	8.0559E+03	3.6351E+03	5.0398E+03	6.1364E+03	2.9024E+03
		SD	4.8144E+02	2.1641E+01	6.11118E+00	2.7044E+02	2.88776E+01	4.4519E+01	6.7395E+02	3.9863E+01	6.9504E+02	4.4174E+02	1.2312E+01
		Min	3.6254E+03	3.4848E+03	3.20964E+03	4.1561E+03	3.20491E+03	3.2946E+03	6.4800E+03	3.5265E+03	4.2319E+03	5.2197E+03	**2.9000E+03**
	100	Avg	9.7476E+03	4.1396E+03	3.26454E+03	8.3674E+03	3.34295E+03	3.6006E+03	1.5131E+04	3.9467E+03	8.0108E+03	1.1094E+04	3.2650E+03
		SD	1.3868E+03	7.7132E+01	1.21219E+01	6.6417E+02	3.72938E+01	8.7639E+01	1.0405E+03	4.3602E+01	1.2072E+03	1.0177E+03	1.2120E+01
		Min	3.7783E+03	4.0418E+03	**3.23900E+03**	7.0448E+03	3.27016E+03	3.4744E+03	1.3013E+04	3.8427E+03	6.1014E+03	8.6071E+03	**3.23900E+03**
F_{28}	30	Avg	6.8198E+03	3.2424E+03	3.10431E+03	5.9172E+03	3.13834E+03	3.2231E+03	7.3960E+03	3.3883E+03	4.8822E+03	5.6745E+03	3.0000E+03
		SD	4.5134E+02	2.5840E+01	6.21026E+00	9.0980E+02	5.39704E+01	1.9100E+01	6.5171E+02	2.7354E+01	4.9009E+02	5.6535E+02	0.0000E+00
		Min	5.9366E+03	3.2216E+03	3.10038E+03	4.6550E+03	3.10000E+03	3.1972E+03	5.3795E+03	3.3383E+03	3.7627E+03	4.7193E+03	**3.0000E+03**
	50	Avg	1.2471E+04	3.3146E+03	3.25885E+03	1.3569E+04	3.27253E+03	3.3007E+03	1.3602E+04	3.8313E+03	8.3397E+03	1.0740E+04	3.0000E+03
		SD	1.8686E+03	2.5497E+01	7.05190E-04	8.3644E+02	2.23841E+01	2.0341E+01	5.4874E+02	7.1347E+01	6.4199E+02	9.6636E+02	0.0000E+00
		Min	3.9310E+03	3.2846E+03	3.25885E+03	1.1475E+04	3.25885E+03	3.2614E+03	1.2233E+04	3.6656E+03	7.1757E+03	8.6012E+03	**3.0000E+03**
	100	Avg	4.2537E+04	3.3340E+03	3.32532E+03	4.4020E+04	3.35855E+03	3.4094E+03	3.6010E+04	5.7440E+03	2.1556E+04	2.9672E+04	**3.3250E+03**
		SD	2.0032E+03	1.4983E+00	2.10549E+01	3.8414E+03	2.52804E+01	4.4405E+01	1.2651E+03	2.7919E+02	2.0743E+03	2.5317E+03	2.1050E+01
		Min	3.7729E+04	3.3303E+03	3.28000E+03	3.7626E+04	3.32422E+03	3.3380E+03	3.1884E+04	5.2986E+03	1.7757E+04	2.4734E+04	**3.2800E+03**
F_{29}	30	Avg	5.0790E+03	3.4795E+03	3.53876E+03	5.3325E+03	3.58602E+03	3.8294E+03	8.7483E+03	3.7058E+03	5.3220E+03	5.5194E+03	3.1000E+03
		SD	2.5445E+02	6.1859E+01	4.80534E+01	3.0235E+02	1.05642E+02	2.3782E+02	1.3978E+03	6.8920E+01	6.5198E+02	6.8858E+02	0.0000E+00
		Min	4.3358E+03	3.3753E+03	3.44510E+03	4.6153E+03	3.38375E+03	3.5027E+03	6.1793E+03	3.5248E+03	4.4793E+03	4.4939E+03	**3.1000E+03**
	50	Avg	1.1922E+04	4.1984E+03	3.88471E+03	8.9666E+03	3.91967E+03	4.7370E+03	1.1286E+05	4.2837E+03	1.2366E+04	1.4918E+04	3.1000E+03
		SD	1.4558E+03	8.7392E+01	7.99824E+01	7.0558E+02	1.67334E+02	4.5021E+02	8.4927E+04	1.1882E+02	3.3076E+03	3.8851E+03	0.0000E+00
		Min	8.6947E+03	4.0024E+03	3.71938E+03	7.8762E+03	3.63802E+03	3.8883E+03	1.6291E+04	4.0836E+03	7.4162E+03	9.2415E+03	**3.1000E+03**
	100	Avg	1.3475E+05	5.7474E+03	6.80880E+03	4.4007E+04	6.95679E+03	8.0784E+03	7.7761E+05	7.0633E+03	3.6932E+04	1.0466E+05	6.7016E+03
		SD	6.5036E+04	2.5808E+02	3.09159E+02	1.3287E+04	2.60364E+02	5.4307E+02	3.0083E+05	2.5985E+02	2.1977E+04	6.9587E+04	4.9977E+02
		Min	5.8723E+04	**5.2684E+03**	6.04704E+03	2.1003E+04	6.47484E+03	7.0846E+03	2.2691E+05	6.4166E+03	1.9128E+04	2.4483E+04	5.7364E+03
F_{30}	30	Avg	3.4349E+08	8.2265E+04	5.15898E+03	1.0872E+08	7.34520E+03	2.4352E+06	2.3060E+09	1.7152E+05	1.3787E+08	6.0064E+07	3.9552E+03
		SD	1.2750E+08	3.3331E+04	2.53753E+01	4.1049E+07	1.14320E+03	1.3621E+06	7.4734E+08	6.8660E+04	9.2673E+07	1.7569E+08	8.4851E+01
		Min	1.5093E+08	2.7593E+04	5.11293E+03	3.9492E+07	5.83005E+03	4.4779E+05	9.7962E+08	8.2110E+04	1.7074E+07	2.7719E+06	**3.8665E+03**
	50	Avg	2.5856E+09	1.9570E+06	5.97396E+05	6.8565E+08	9.12600E+05	3.7337E+07	8.2333E+09	9.2960E+06	8.0426E+08	5.6348E+08	8.9103E+03
		SD	6.1016E+08	9.8413E+05	3.69478E+03	1.8614E+08	1.50551E+05	6.3925E+06	1.9703E+09	1.5446E+06	4.3487E+08	1.3970E+09	3.8719E+02
		Min	1.3616E+09	6.5975E+05	5.91366E+05	3.2624E+08	7.42009E+05	2.6137E+07	5.1460E+09	5.5808E+06	2.7722E+08	1.6178E+08	**8.3742E+03**
	100	Avg	2.1579E+10	3.2964E+04	5.33307E+03	1.2979E+10	9.38505E+03	2.0292E+07	4.2111E+10	8.7544E+06	7.9595E+09	2.6654E+10	6.5650E+03
		SD	5.4514E+09	2.3227E+04	8.87996E+01	1.9913E+09	3.20617E+03	7.4220E+06	3.4559E+09	1.9504E+06	3.2648E+09	5.7806E+09	1.0082E+02
		Min	1.0733E+08	9.6963E+03	**5.18486E+03**	9.4484E+09	6.13794E+03	7.9235E+06	3.3669E+10	5.1366E+06	3.7797E+09	1.6889E+10	6.4206E+03
Ranking	**30**	**W|T|L**	0|0|10	0|0|10	0|0|10	0|0|10	0|0|10	0|1|9	0|0|10	0|0|10	0|0|10	0|0|10	**10|0|0**
	50	**W|T|L**	0|0|10	0|0|10	1|0|9	0|0|10	0|0|10	0|0|10	0|0|10	0|0|10	0|0|10	0|0|10	**9|0|1**
	100	**W|T|L**	0|0|10	1|2|7	1|1|8	0|0|10	0|0|10	1|0|9	0|0|10	0|0|10	0|0|10	0|0|10	**5|3|2**

5.3.3 Evaluation of convergence speed

In this experiment set, the convergence speed of the proposed QANA was assessed, and the results were compared with the contender algorithms. For such comparisons, the convergence curves of the best fitness values obtained by each algorithm in different dimensions 30, 50, and 100 are plotted in Fig. 10 for test functions unimodal and multimodal and in Fig. 11 for test functions hybrid and composition. For most test functions, the QANA shows a common behavior in which the search agents with a steep descent slope converge toward promising regions in the initial iterations. This is because the QANA can effectively explore the landscape using the multi-flock and qubit-crossover operator, which enhances the diversity and landscape coverage. Then, in the next iterations, the QANA can converge toward better solutions because it can percept the landscape of different problems using the visited positions stored by LTM and STM and assign the suitable mutation strategy to flocks based on their success rate. In the final iterations, the search agents are greedily moved toward the optimum solutions using the V-echelon communication topology in which the search agents follow their front member.

To sum up, the obtained results from the unimodal, multimodal, hybrid, and composition test functions demonstrate that the QANA is superior to the other algorithms and has outstanding exploitation and exploration abilities for unimodal test functions F_1 and F_3 and multimodal test functions F_5, F_7, and F_{10}. Moreover, the convergence curves plotted for the test functions $\{F_{12}, F_{16}, F_{23}, F_{24}, F_{29}, F_{30}\}$ show that the proposed algorithm can bypass the local optima by striking between its exploration and exploitation abilities.

5.3.4 Scalability evaluation

Most existing differential evolutionary algorithms have no sufficient mechanism to cope with the curse of dimensionality, which results in decreased exploration ability and increased cost of convergence to any local optima (LaTorre et al., 2013; Maučec and Brest, 2019). Therefore, we designed this section to evaluate the scalability of the QANA for solving large-scale global optimization (LSGO) problems. The CEC 2013 LSGO benchmark functions (Li et al., 2013), including 15 complex functions, with dimensions 1000, were considered, and the QANA and other competitor algorithms were applied to solve its functions over 30 independent runs. The algorithms set the number of population and maximum function evaluations (MaxFEs) to 200 and $D \times 10^3$, respectively. Table 5 presents the comparison results in terms of the standard statistical metrics, including Avg, SD, and Min, and the convergence curves of scalability are plotted in Fig. 12. The experimental results show that the QANA can better cope with the dimensionality problem and is more scalable than other contender algorithms for solving these extremely high-dimensional problems. This is attributable to the V-echelon topology and LTM and STM of QANA to find the promising regions greedily and store useful solutions gained by previous iterations, respectively. The algorithm is also capable of adequate search space coverage in high-dimensional problems. Moreover, the proposed algorithm is equipped with the qubit-crossover operator, which maintains the diversity and inhibits greediness.

5.3.5 Performance index (PI) analysis

The performance index (PI) (Deep and Thakur, 2007) is a criterion to show the relative performance of different algorithms in terms of their effectiveness and computational time (Gupta and Deep, 2019). The PI of the i-th algorithm is determined using Eq. (15), where the parameter Mf^j is the minimum average error value obtained by all the algorithms for the j-th function, and Af^j is the average error value obtained by an algorithm for the j-th function. Also, Mt^j is the minimum of average time used by all the algorithm for the j-th function, At^j is the average time used by an algorithm for the j-th function, and parameter N_F is the total number of test functions. The parameters α and β (α + β =1 and α, β are between intervals [0, 1]) are the weights assigned to the error value and computational time, respectively. The criteria PI for α = ω and β = 1 − ω where ω = [0, 0.2, 0.4, 0.6, 0.8 and 1] is evaluated and plotted in Fig. 13.

$$PI_i = \frac{1}{N_F}\sum_{j=1}^{N_F}(\alpha \times \frac{Mf^j}{Af^j} + \beta \times \frac{Mt^j}{At^j}) \tag{15}$$

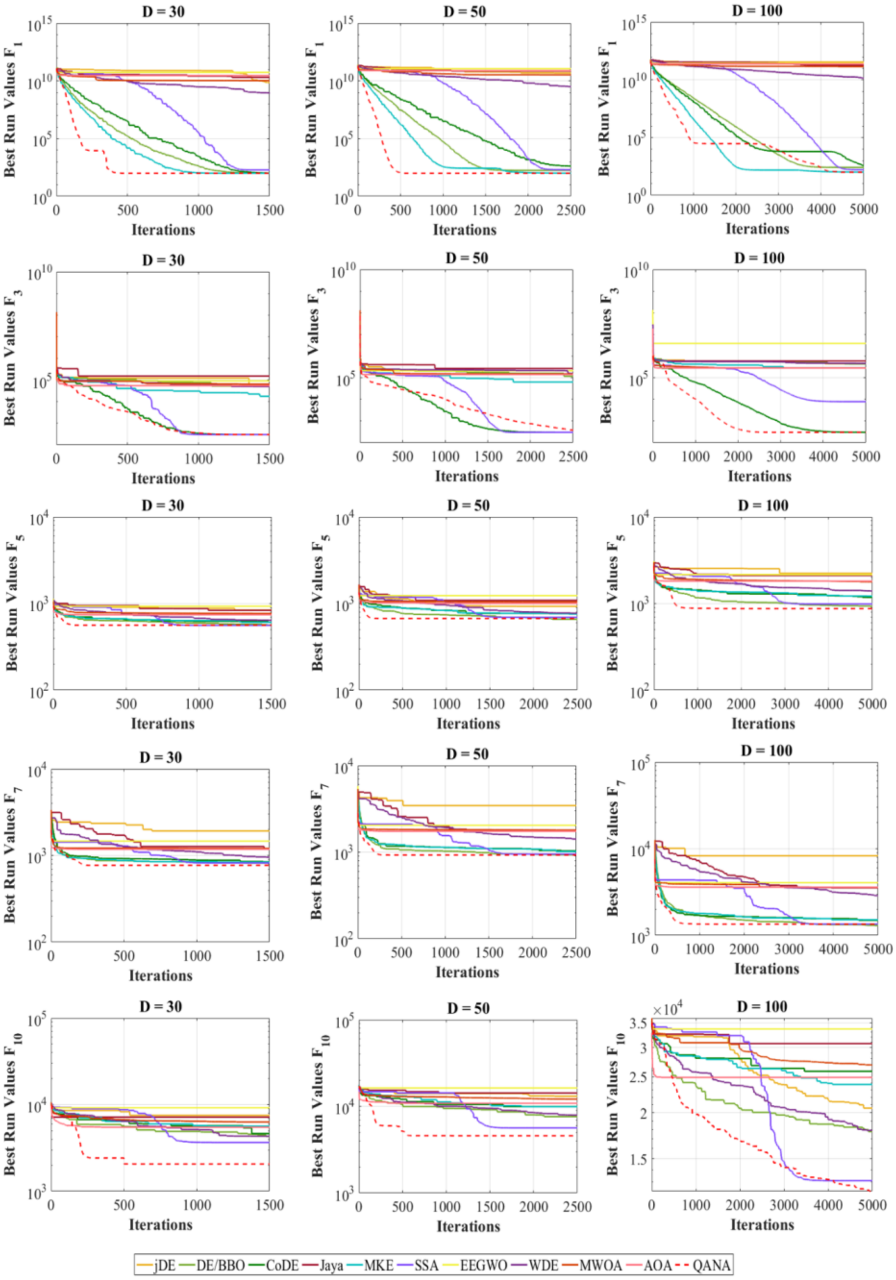

Fig. 10 Comparison of convergence curves of algorithms in unimodal and multimodal test functions.

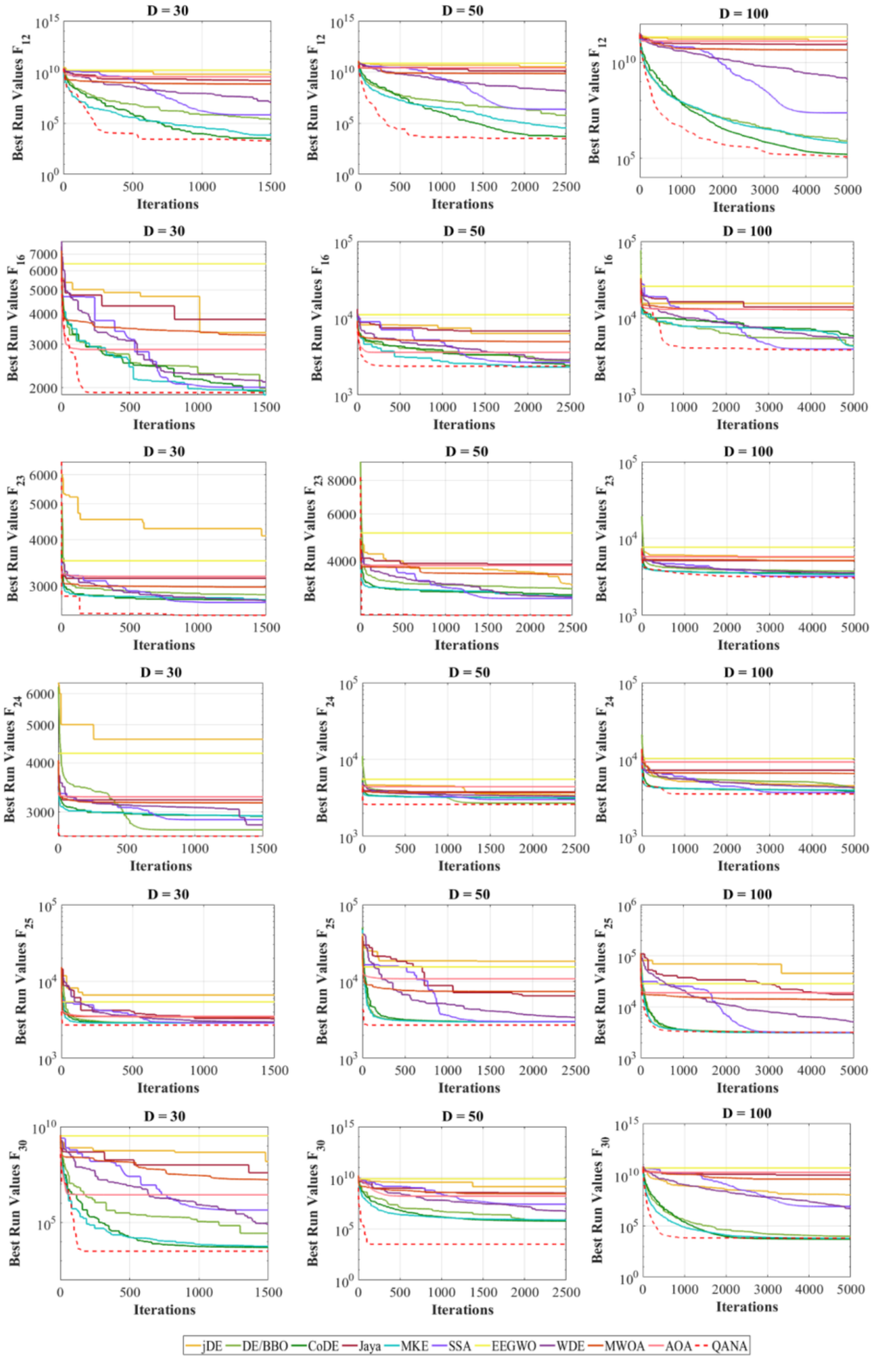

Fig. 11 Comparison of convergence curves of algorithms in hybrid and composition test functions.

Table 5 Comparison of optimization results for LSGO problems using CEC 2013 with D = 1000.

Func.	Metrics	jDE (2006)	DE/BBO (2010)	CoDE (2011)	Jaya (2016)	MKE (2016)	SSA (2017)	EEGWO (2018)	WDE (2018)	MWOA (2018)	AOA (2021)	QANA
F_1	Avg	2.61300E+11	1.92948E+08	7.57297E+06	2.19727E+11	1.60759E+08	2.64911E+09	1.97500E+11	6.38900E+10	2.00500E+11	1.92124E+11	2.60700E+05
	SD	4.97500E+10	7.43773E+06	6.67791E+05	1.32474E+10	7.40734E+07	2.19535E+08	2.48200E+09	2.25900E+09	4.21100E+09	5.77470E+09	1.07400E+05
	Min	2.52000E+10	1.84198E+08	6.59147E+06	1.93830E+11	8.42055E+07	2.34829E+09	1.91500E+11	5.85900E+10	1.92600E+11	1.80878E+11	**8.50800E+04**
F_2	Avg	8.91600E+04	7.55322E+03	1.05212E+04	9.18752E+04	2.53862E+04	2.68757E+04	4.68600E+04	4.59900E+04	4.29100E+04	4.67639E+04	6.05500E+03
	SD	1.19400E+04	1.56660E+02	1.48559E+02	1.87184E+04	1.33691E+03	1.51166E+03	1.86600E+02	8.04200E+02	1.82100E+02	2.98864E+02	2.78600E+02
	Min	3.26700E+04	7.34270E+03	1.01714E+04	6.63080E+04	2.32291E+04	2.43447E+04	4.63400E+04	4.40500E+04	4.25900E+04	4.60221E+04	**5.45800E+03**
F_3	Avg	2.14100E+01	2.06977E+01	2.36487E+00	2.15838E+01	1.98935E+01	1.94643E+01	2.10400E+01	2.11500E+01	2.10600E+01	2.15871E+01	6.34100E+00
	SD	2.07000E-01	1.54691E-02	1.05771E-01	6.46945E-03	8.45809E-02	1.49844E-02	9.39900E-03	1.07800E-02	1.47300E-02	1.34033E-02	3.18500E-01
	Min	2.04100E+01	2.06755E+01	**2.19962E+00**	2.15750E+01	1.97644E+01	1.94420E+01	2.10100E+01	2.11200E+01	2.10300E+01	2.15611E+01	5.93300E+00
F_4	Avg	5.80800E+12	3.38809E+11	1.09217E+10	7.63708E+12	3.75175E+10	3.07581E+11	1.63900E+13	5.36600E+11	1.16000E+13	4.32093E+12	2.98900E+09
	SD	7.68800E+11	6.03759E+10	3.58317E+09	1.36970E+12	1.40717E+10	2.80569E+10	3.90200E+12	4.26900E+10	4.96300E+12	2.46035E+12	7.16900E+08
	Min	4.09600E+12	2.20823E+11	5.72711E+09	5.50368E+12	1.43117E+10	2.55970E+11	8.40600E+12	4.42400E+11	4.32900E+12	1.84734E+12	**1.77500E+09**
F_5	Avg	4.28000E+07	5.84221E+06	5.14902E+06	3.76329E+07	4.23234E+06	8.48878E+06	4.15400E+07	1.72700E+07	4.26900E+07	3.43114E+07	2.92400E+06
	SD	5.66300E+06	2.13648E+05	1.11370E+06	3.97479E+06	8.90745E+05	1.49783E+06	1.06800E+06	8.02700E+05	2.90900E+06	2.30091E+06	3.59300E+05
	Min	1.73300E+07	5.43052E+06	2.41119E+06	3.29415E+07	2.70691E+06	6.51480E+06	3.84400E+07	1.55500E+07	3.43600E+07	3.08441E+07	**2.11300E+06**
F_6	Avg	1.04600E+06	1.05936E+06	3.02237E+01	1.06191E+06	1.18986E+05	3.65256E+05	1.03000E+06	1.01400E+06	1.03300E+06	1.06120E+06	5.57700E+03
	SD	2.17900E+03	2.01087E+03	1.26204E+00	8.03500E+02	1.64202E+04	4.08725E+05	1.44300E+03	6.33500E+03	2.75400E+03	2.04005E+03	3.92900E+01
	Min	1.04000E+06	1.05618E+06	**2.82614E+01**	1.06009E+06	8.92024E+04	7.89241E+04	1.02600E+06	9.99000E+05	1.02800E+06	1.05523E+06	5.48900E+03
F_7	Avg	2.57100E+14	2.95032E+09	1.91320E+09	4.54913E+14	4.54755E+08	5.92964E+08	1.72500E+14	9.93400E+10	2.83100E+14	7.31503E+13	6.44300E+06
	SD	1.01800E+14	5.79138E+08	4.23791E+08	2.25031E+14	2.58237E+08	2.67191E+08	4.01900E+13	1.88400E+10	1.25200E+14	3.58885E+13	1.51600E+06
	Min	8.91600E+09	2.33212E+09	1.06265E+09	1.78146E+14	1.92894E+08	3.49917E+08	6.96000E+13	6.59000E+10	8.64800E+13	2.19834E+13	**3.85300E+06**
F_8	Avg	2.39400E+17	9.63505E+15	3.29413E+11	1.59153E+16	1.08873E+14	6.57748E+14	8.01900E+17	2.44800E+15	4.82800E+17	2.23875E+16	1.18700E+12
	SD	5.52700E+16	1.48983E+13	1.67017E+11	2.22176E+16	5.53310E+13	1.69666E+14	2.13900E+17	5.95000E+14	1.80500E+17	9.17163E+15	9.63700E+11
	Min	1.20100E+17	7.24856E+15	1.87505E+11	7.26489E+16	3.68859E+13	4.12290E+14	3.19600E+17	1.06400E+15	2.69400E+17	5.38412E+16	**1.28000E+11**
F_9	Avg	3.29900E+09	4.44818E+08	1.87738E+08	3.92337E+09	3.25516E+08	8.24005E+08	3.69500E+09	1.28600E+09	3.47600E+09	2.67995E+09	2.97600E+08
	SD	2.15800E+08	3.64608E+07	7.64609E+07	2.17044E+08	6.44244E+07	1.29589E+08	2.17200E+08	5.98900E+07	3.21100E+08	3.06751E+08	1.93700E+07
	Min	2.66600E+09	3.85317E+08	**1.24010E+08**	3.67943E+09	2.32493E+08	6.30737E+08	3.19100E+09	1.14300E+09	2.73200E+09	2.12716E+09	2.65300E+08
F_{10}	Avg	8.65900E+07	9.40538E+07	1.05133E+03	9.43948E+07	3.85343E+05	3.94886E+06	9.30400E+07	2.87500E+07	9.34300E+07	9.39159E+07	4.88100E+04
	SD	1.11900E+07	1.70388E+05	3.18889E+01	8.41805E+04	5.62682E+05	4.41290E+06	4.32200E+05	1.81700E+06	8.64400E+05	3.35281E+05	5.30600E+02
	Min	3.32900E+07	9.38328E+07	9.93642E+02	9.42732E+07	**2.05443E+03**	1.32314E+06	9.19700E+07	2.55000E+07	9.07400E+07	9.33563E+07	4.65900E+04
F_{11}	Avg	1.95300E+16	3.01974E+11	5.34862E+10	1.27604E+16	1.62624E+11	8.19634E+09	7.72800E+15	3.98500E+13	7.70800E+15	2.84556E+15	3.61900E+08
	SD	5.46800E+15	8.17347E+10	1.52041E+10	7.97606E+15	1.01385E+11	2.29325E+09	2.01200E+15	8.05400E+12	3.57900E+15	1.10165E+15	9.50200E+07
	Min	8.38800E+15	1.62215E+11	2.68130E+10	3.62977E+15	3.97159E+10	6.05133E+09	4.04700E+15	2.15600E+13	2.60800E+15	1.18220E+15	**2.14800E+08**
F_{12}	Avg	6.25100E+12	8.66714E+09	3.93143E+06	2.39853E+12	3.84993E+10	7.75168E+06	1.68800E+12	2.72900E+12	1.70300E+12	1.68326E+12	1.78600E+04
	SD	1.00900E+12	1.06837E+09	1.13619E+06	6.01118E+10	8.80314E+09	2.30220E+06	6.06300E+09	9.32500E+10	7.06500E+09	7.31024E+09	6.32600E+04
	Min	1.65600E+12	7.41119E+09	2.12935E+06	2.28890E+12	2.49192E+10	4.44575E+06	1.67400E+12	2.48400E+12	1.68700E+12	1.67044E+12	**3.16500E+03**
F_{13}	Avg	2.21800E+16	7.65865E+10	3.25557E+10	1.29350E+17	1.62132E+10	1.71877E+10	1.54600E+16	3.37000E+13	9.31000E+15	6.01586E+15	8.60700E+08
	SD	6.36100E+15	1.34787E+10	8.87535E+09	7.56567E+16	5.06498E+09	3.75750E+09	3.66000E+15	8.50200E+12	3.70100E+15	3.93141E+15	3.79700E+08
	Min	1.05800E+16	5.60574E+10	2.00304E+10	4.79093E+16	9.42411E+09	1.31282E+10	9.61500E+15	1.60100E+13	3.22100E+15	8.06022E+14	**3.99800E+08**
F_{14}	Avg	3.44100E+16	1.00230E+12	7.99067E+10	3.82489E+16	3.00138E+11	1.05850E+11	2.66600E+16	6.19400E+13	3.66100E+16	6.77208E+15	2.66100E+08
	SD	9.05100E+15	1.78673E+11	2.25045E+10	3.87454E+16	1.23358E+11	4.08356E+10	8.73900E+15	1.52800E+13	2.12200E+16	4.53939E+14	1.72100E+08
	Min	2.05500E+16	6.63593E+11	3.98786E+10	9.82674E+15	9.88885E+10	5.15579E+10	1.21800E+16	3.61300E+13	8.53600E+15	2.45994E+15	**6.84300E+07**
F_{15}	Avg	5.04200E+16	1.00182E+08	2.22929E+08	1.37919E+16	5.64352E+07	3.00632E+07	1.82300E+15	1.56800E+14	2.49600E+11	1.11375E+15	4.15200E+06
	SD	1.62400E+16	6.84632E+06	3.16517E+07	6.79353E+15	3.44933E+07	3.15888E+06	1.35500E+14	1.93800E+13	4.31400E+10	8.76659E+13	5.77300E+05
	Min	1.67200E+13	8.47221E+07	1.60899E+08	8.07592E+15	2.44351E+07	2.55108E+07	1.49600E+15	1.01400E+14	1.40100E+11	9.84959E+14	**3.32100E+06**
Ranking	**W|T|L**	0|0|15	0|0|15	3|0|12	0|0|15	1|0|14	0|0|15	0|0|15	0|0|15	0|0|15	0|0|15	**11|0|4**

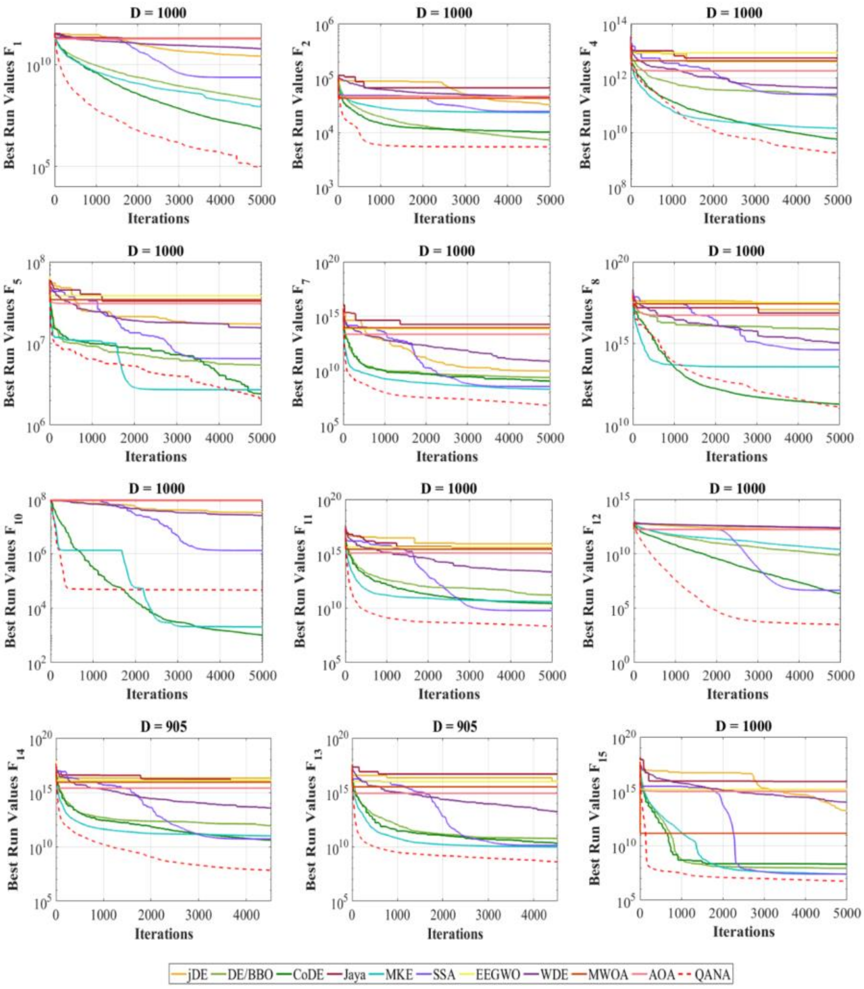

Fig. 12 Comparison of convergence curves for LSGO problems using CEC 2013 with D = 1000.

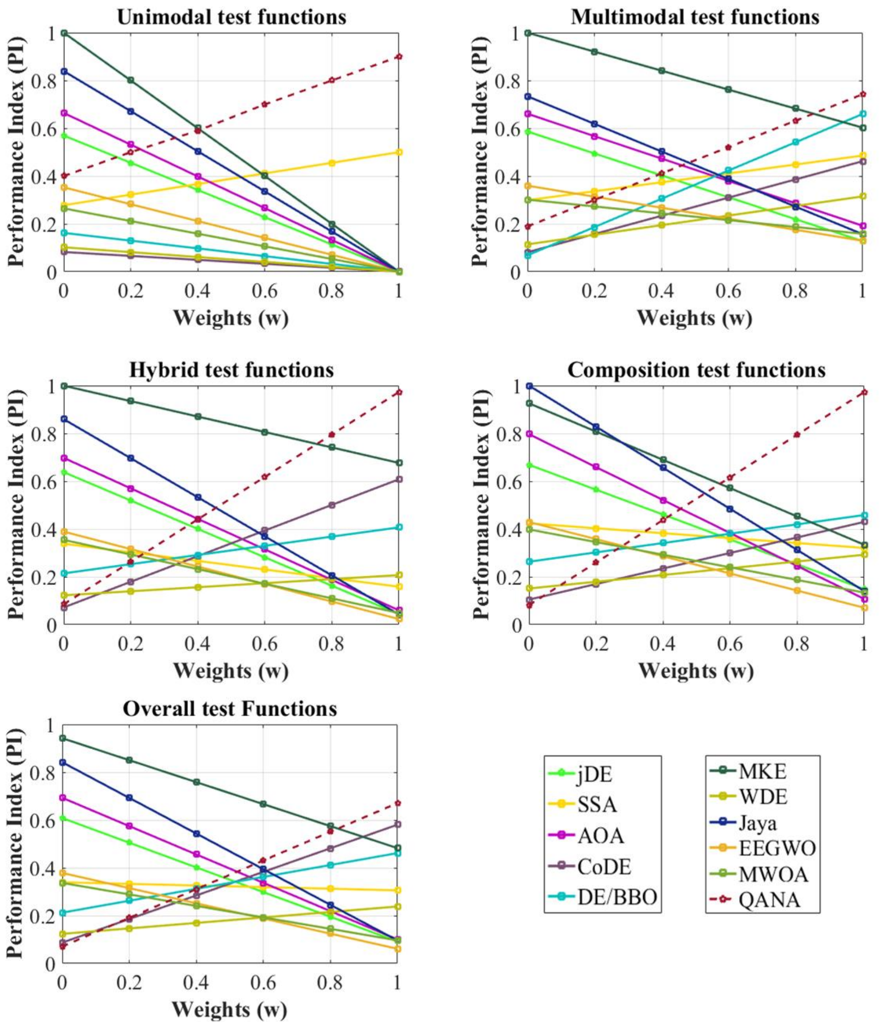

Fig. 13 Performance index (PI) analysis

5.4. Non-parametric statistical test analysis

To statistically prove the superiority of the QANA, the experimental results were analyzed by three statistical tests, i.e. Wilcoxon signed-rank sum (Wilcoxon, 1992), analysis of variance (ANOVA), and mean absolute error (MAE).

5.4.1. Wilcoxon signed-rank test

The Wilcoxon signed-rank test is a more sensitive non-parametric test, which is computed by considering the best solutions obtained by each algorithm for the corresponding test function during 30 independent runs. In this test, a p-value with a 95% significance level (α = 0.05) was computed, and the corresponding results for dimensions 30, 50, and 100 are reported in Table

6, in which the symbol '>' indicates that the proposed algorithm is significantly better than the compared algorithm.

Table 6 Wilcoxon's signed-ranks test ($p \geq 0.05$).

Functions	Unimodal test functions		Multimodal test functions		Hybrid test functions		Composition test functions	
Algorithms	p-value	Sig.	p-value	Sig.	p-value	Sig.	p-value	Sig.
QANA vs. jDE	2.121E-54	>	1.729E-62	>	1.496E-182	>	1.398E-138	>
QANA vs. DE/BBO	7.091E-22	>	4.515E-03	>	2.257E-14	>	2.300E-14	>
QANA vs. CoDE	2.264E-02	>	4.963E-02	>	1.282E-27	>	8.179E-39	>
QANA vs. Jaya	3.412E-48	>	1.508E-47	>	1.828E-163	>	3.822E-132	>
QANA vs. MKE	2.366E-06	>	8.838E-02	>	3.197E-02	>	3.044E-46	>
QANA vs. SSA	1.605E-07	>	1.540E-03	>	6.255E-69	>	1.033E-35	>
QANA vs. EEGWO	2.495E-54	>	1.329E-61	>	2.422E-200	>	6.400E-180	>
QANA vs. WDE	1.149E-59	>	3.411E-22	>	9.044E-112	>	1.854E-84	>
QANA vs. AAO	2.808E-59	>	1.664E-53	>	2.185E-163	>	8.782E-172	>
QANA vs. MWOA	4.526E-54	>	1.331E-51	>	1.466E-170	>	7.070E-149	>

5.4.2. ANOVA test

The analysis of variance (ANOVA) test has been conducted with a 5% significance level to highlight the consistency and overall performance of the results obtained by the comparative algorithms. The data obtained from 30 runs were performed for the ANOVA test, and the results are plotted in Figs. 14 and 15 for different dimensionsm 30, 50, and 100. These results prove that the proposed QANA is superior to the contender algorithm in terms of analysis of variance.

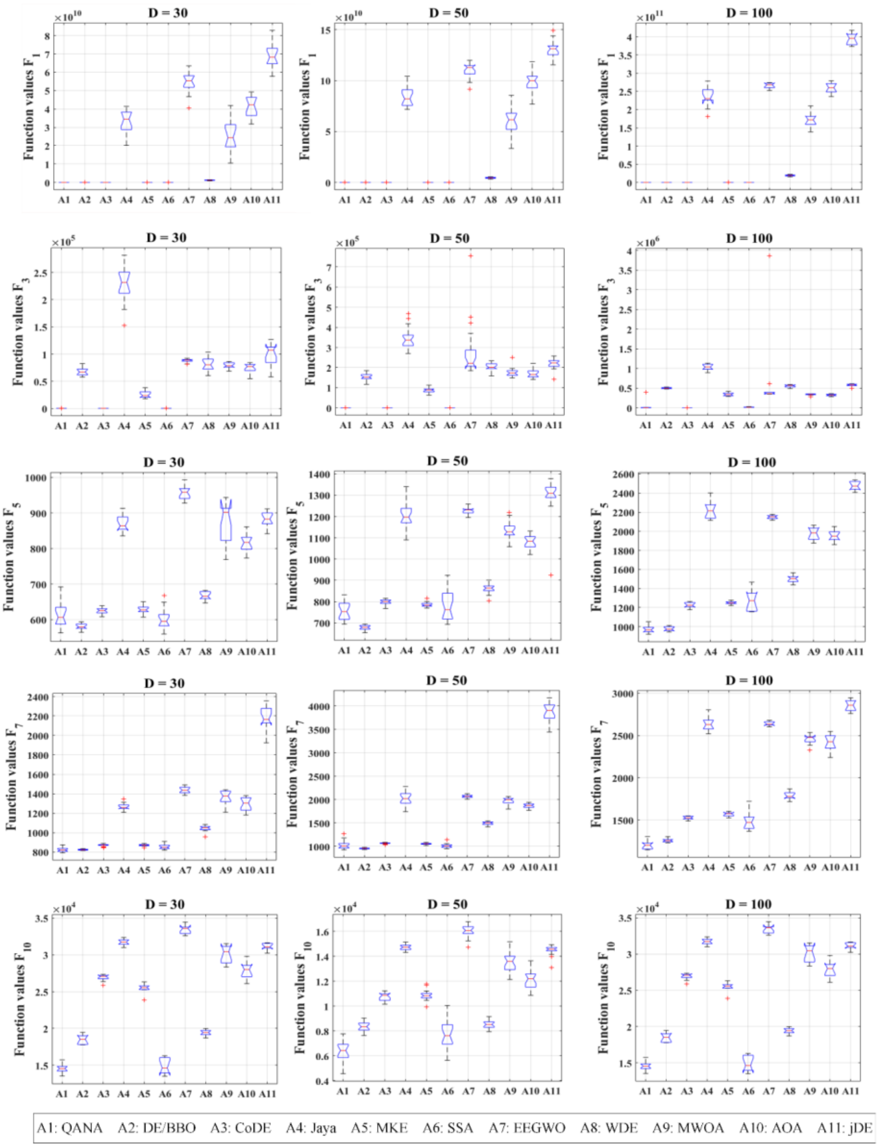

Fig. 14 ANOVA test in unimodal and multimodal test functions.

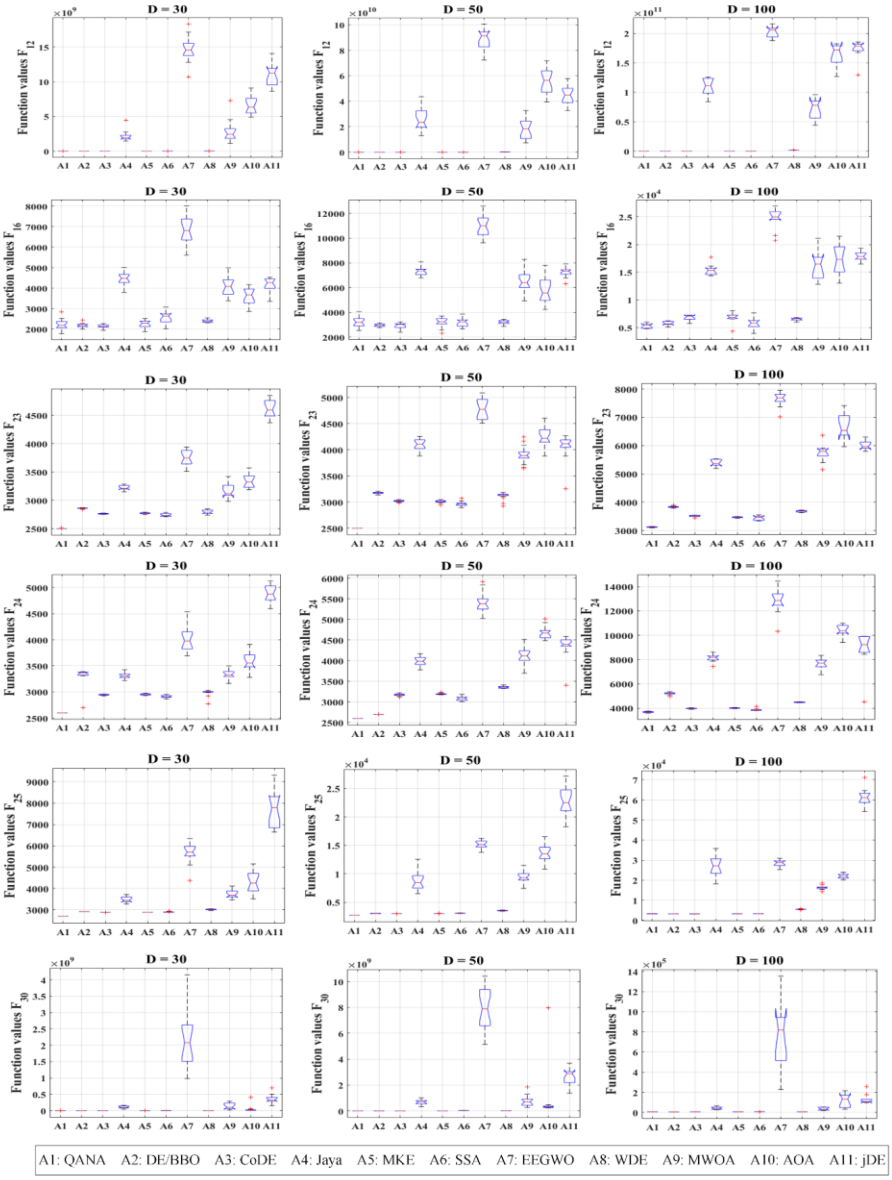

Fig. 15 ANOVA test in hybrid and composition test functions.

5.4.3. Mean absolute error (MAE)

Moreover, the solutions gained by all algorithms were analyzed using the mean absolute error (MAE) to determine the difference between the estimated and optimal solutions. Tables 7 and 8 provide the MAE results for benchmark functions CEC 2018 with dimensions 30, 50, 100, and CEC 2013 with dimension 1000 for LSGO problems, respectively. The MAE was separately computed for each algorithm using Eq. (16), where the parameter NF is the number of functions, O_j and Y_j are the global optimum solution and the best result obtained in the j-th function, respectively.

$$MAE = \frac{\sum_{j=1}^{N_f} |O_j - Y_j|}{N_f} \tag{16}$$

Table 7 MAE test of the algorithms on all benchmark functions of CEC 2018 with different dimensions.

Unimodal test functions						
Algorithms	MAE D=30	Rank D=30	MAE D=50	Rank D=50	MAE D=100	Rank D=100
jDE	3.620E+09	8	2.423E+10	9	1.751E+11	11
DE/BBO	2.612E+04	5	5.849E+04	5	2.169E+05	5
CoDE	1.819E+00	2	1.586E+02	3	7.988E+02	2
Jaya	1.006E+10	9	3.586E+10	8	9.050E+10	8
MKE	8.790E+03	4	3.156E+04	4	1.431E+05	4
SSA	4.724E+01	3	5.236E+01	2	3.815E+03	3
EEGWO	2.030E+10	11	4.581E+10	11	1.262E+11	10
WDE	4.026E+08	6	1.576E+09	6	6.934E+09	6
MWOA	5.267E+09	7	1.671E+10	7	6.940E+10	7
AOA	1.438E+10	10	3.846E+10	10	1.180E+11	9
QANA	**1.212E-05**	**1**	5.427E-01	**1**	1.296E+02	**1**
Multimodal test functions						
Algorithms	MAE D=30	Rank D=30	MAE D=50	Rank D=50	MAE D=100	Rank D=100
jDE	3.003E+03	10	3.620E+03	7	3.2501E+04	11
DE/BBO	5.169E+02	3	1.038E+03	2	3.3329E+03	2
CoDE	5.795E+02	4	1.405E+03	5	3.8887E+03	4
Jaya	2.550E+03	9	8.314E+03	10	2.4829E+04	9
MKE	7.143E+02	5	1.395E+03	4	3.6010E+03	3
SSA	4.371E+02	2	1.188E+03	3	4.3188E+03	5
EEGWO	4.638E+03	11	1.196E+04	11	2.8348E+04	10
WDE	9.949E+02	6	2.694E+03	6	9.2517E+03	6
MWOA	1.557E+03	8	5.856E+03	8	1.6938E+04	7
AOA	1.529E+03	7	6.189E+03	9	1.7712E+04	8
QANA	**2.583E+02**	**1**	**6.353E+02**	**1**	**2.6596E+03**	**1**
Hybrid test functions						
Algorithms	MAE D=30	Rank D=30	MAE D=50	Rank D=50	MAE D=100	Rank D=100
jDE	6.477E+08	10	3.583E+09	10	1.308E+10	9
DE/BBO	3.291E+04	4	1.120E+05	4	6.065E+05	4
CoDE	2.355E+02	2	8.284E+02	2	1.705E+04	2
Jaya	1.578E+08	8	2.138E+09	8	1.090E+10	8
MKE	6.486E+02	3	3.678E+03	3	6.859E+04	3
SSA	1.043E+05	5	2.710E+05	5	2.544E+06	5
EEGWO	1.549E+09	11	1.068E+10	11	2.678E+10	11
WDE	1.166E+06	6	1.439E+07	6	1.235E+08	6
MWOA	6.826E+07	7	7.848E+08	7	4.960E+09	7
AOA	3.454E+08	9	2.582E+09	9	1.556E+10	20
QANA	**1.550E+02**	**1**	**6.437E+02**	**1**	**6.939E+03**	**1**
Composition test functions						
Algorithms	MAE D=30	Rank D=30	MAE D=50	Rank D=50	MAE D=100	Rank D=100
jDE	1.509E+07	10	1.362E+08	10	1.075E+07	7
DE/BBO	2.995E+03	4	6.653E+04	3	2.618E+03	3
CoDE	5.516E+02	2	5.961E+04	2	1.784E+03	2
Jaya	3.951E+06	9	3.263E+07	9	9.449E+08	9
MKE	7.838E+02	3	7.565E+04	4	4.537E+03	4
SSA	4.480E+04	6	2.614E+06	6	7.944E+05	6
EEGWO	9.797E+07	11	5.146E+08	11	3.367E+09	11
WDE	8.376E+03	5	5.588E+05	5	5.175E+05	5
MWOA	1.708E+06	8	2.773E+07	8	3.780E+08	8
AOA	2.784E+05	7	1.618E+07	7	1.689E+09	10
QANA	**1.648E+02**	**1**	**1.796E+02**	**1**	**8.954E+02**	**1**

Table 8 MAE test of the algorithms for CEC2013 LSGO benchmark functions with dimension 1000.

Algorithms	MAE D=1000	Rank D=1000
jDE	1.064E+16	9
DE/BBO	4.833E+14	6
CoDE	1.875E+10	2
Jaya	9.485E+15	8
MKE	2.472E+12	3
SSA	2.751E+13	4
EEGWO	2.313E+16	11
WDE	8.283E+13	5
MWOA	1.892E+16	10
AOA	3.953E+15	7
QANA	**8.715E+09**	**1**

6. Applicability of QANA for solving engineering design problems

Many engineering problems are non-linear and constrained, and constraints handling refers to optimize the objective functions under given constraints for finding a feasible solution. In this regard, the ability of the proposed QANA for solving real-world optimization problems was evaluated by four engineering problems, i.e. tension/compression spring design, pressure vessel design (PVD), three-bar truss design, and welded beam design (WBD). The details of these problems and their objective functions are described in Appendix A. To achieve a fair comparison, the QANA and competitor algorithms were executed for 30 different runs. For each problem, the parameter values of the maximum number of function evaluations (FEs) and the population size were set to $D\times10^4$ and 50, respectively. The results were compared with other state-of-the-art algorithms and are reported in Tables 9–12. The convergence curves of the QANA for solving four engineering problems are shown in Fig. 16.

Table 9 Results for tension/compression spring design problem.

Algorithms	Optimal values for variables			Optimum weight
	d	D	N	
jDE	0.054034	0.407561	10.127434	0.01292947
DE/BBO	0.060303	0.494159	10.183030	0.02189302
CoDE	0.050264	0.319697	14.080980	0.01298961
Jaya	0.051786	0.359045	11.155078	0.01266690
MKE	0.052466	0.375666	10.269711	0.01268829
SSA	0.052309	0.371823	10.455412	0.01267218
EEGWO	0.071251	0.536728	13.131940	0.04123091
WDE	0.056750	0.437036	12.765199	0.02078208
MWOA	0.054426	0.426187	8.161806	0.01282989
AOA	0.050000	0.317385	14.553272	0.01313439
QANA	0.051926	0.362432	10.961632	**0.01266625**

Table 10 Results for pressure vessel design problem.

Algorithms	Optimal values for variables				Optimum cost
	T_s	T_h	R	L	
jDE	1.4393774	0.724791	67.222723	10.400860	9.28148547E+03
DE/BBO	1.7932330	2.298101	45.390909	141.259836	1.99095329E+04
CoDE	0.881838	0.449011	43.051343	168.197626	6.53240702E+03
Jaya	0.7786234	0.384867	40.328601	199.902730	5.88864507E+03
MKE	0.7781692	0.384649	40.319619	200.000000	5.88533302E+03
SSA	0.7789012	0.385012	40.357569	199.472410	5.88659056E+03
EEGWO	3.0393982	2.180589	78.557921	18.023585	4.15319882E+04
WDE	94.711664	20.61617	33.372093	186.702264	1.47055154E+04
MWOA	0.8755801	0.433644	45.365979	140.422871	6.08939785E+03
AOA	0.8252370	0.502613	40.925818	200.000000	6.68519215E+03
QANA	0.7781687	0.384649	40.319619	200.000000	**5.88533277E+03**

Table 11 Results for the three-bar truss problem

Algorithms	Optimal values for variables		Optimal weight
	x_1	x_2	
jDE	0.790449	0.403527	2.638990006E+02
DE/BBO	0.763495	0.492169	2.651657308E+02
CoDE	0.787621	0.411279	2.639008002E+02
Jaya	0.788627	0.408385	2.6389585121E+02
MKE	0.791907	0.399584	2.639435001E+02
SSA	0.788678	0.408241	2.63895843382E+02
EEGWO	0.806439	0.368564	2.649516916E+02
WDE	0.454766	0.651664	2.641254239E+02
MWOA	0.789961	0.404649	2.638995223E+02
AOA	0.789605	0.405664	2.639004316E+02
QANA	0.788675	0.408248	**2.63895843376E+02**

Table 12 Results of the welded beam design problem

Algorithms	Optimal values for variables				Optimum cost
	h	l	t	b	
jDE	0.573662	4.361220	2.352191	0.429303	1.876631
DE/BBO	0.198546	3.978957	8.794421	0.271069	2.235268
CoDE	0.200068	3.575454	9.226260	0.206701	1.770640
Jaya	0.205746	3.470675	9.036149	0.205754	1.725004
MKE	0.205729	3.470548	9.036550	0.205734	1.724876
SSA	0.205582	3.473672	9.036625	0.205730	1.725053
EEGWO	0.268139	6.563012	7.950610	0.355915	3.320707
WDE	0.255666	3.516591	8.192765	0.275378	2.155207
MWOA	0.200578	3.597398	9.005897	0.209362	1.756161
AOA	0.195824	3.735867	10.00000	0.201829	1.880410
QANA	0.205730	3.470489	9.036624	0.205730	**1.724852**

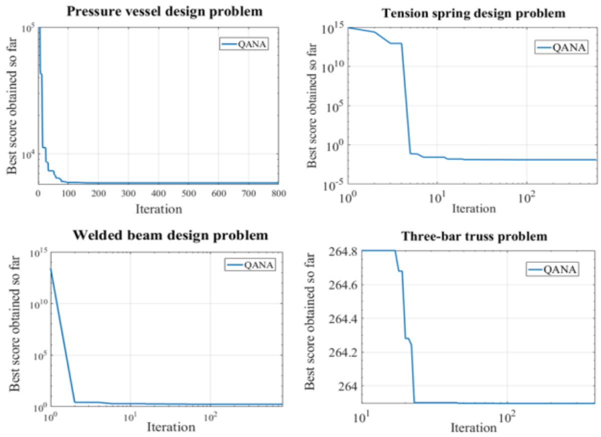

Fig. 16 Convergence curves of QANA for solving engineering design problems.

7. Discussion

In this section, the main reasons for the proposed QANA algorithm's superiority over the contender algorithms are discussed. The experimental results demonstrate that the QANA algorithm can be effectively adapted for various problems by applying its V-echelon communication topology, success-based population distribution (SPD) policy, mutation strategies, LTM and STM memories, and a qubit-crossover operator.

From the qualitative results plotted in Fig. 6 and 7, the search agents can effectively cover the search space and finally converge to the promising area. The result of the population diversity analysis in Fig. 8 shows that QANA can maintain diversity during the search process. The main reason is that the LTM and STM memories store previous experience solutions, which are then used in two mutation strategies, DE/quantum/I and DE/quantum/II. Subsequently, the exploration ability is increased and suspends the premature convergence before finding a more promising area. The exploration and exploitation analysis plotted in Fig. 9 proves that QANA devotes a high percentage of exploitation in unimodal test functions and a high percentage of exploration in multimodal test functions. This ability can be attributed to the use of Eqs. (2) and (3) which are exploitation-oriented and Eq. (4) that is exploration-oriented. Moreover, QANA can effectively switch between exploration and exploitation in hybrid and composition test functions using the success-based population distribution (SPD) policy.

From the results and curves presented in Table 2 and Fig. 10, the QANA algorithm is competitive for unimodal and multimodal test functions by converging to the promising area accurately in terms of its exploitation and exploration abilities. This can further be attributed to the V-echelon topology introduced in Definition 3, which promotes information flow using informative disciplines for headers and followers in each flock. The experimental evaluations reported in Tables 3 and 4 and convergence curves in Fig. 11 prove that the SPD policy proposed in Definition 4 could enrich the flocks by assigning the proper mutation strategies based on their improvement rate. The scalability results reported in Table 5 and convergence curves in Fig. 12 prove that QANA is superior to the contender algorithms. This is supported by the division of the population into several flocks to explore the problem space independently, while the self-adaptive quantum orientation proposed in Definition 5 can produce and maintain the best parameters values obtained by success solutions. Moreover, the qubit-crossover probability proposed in Definition 6 combines the new and old generations to increase diversity and focus on exploitation.

8. Conclusion and future work

This study proposes a novel, differential evolution (DE) algorithm named QANA, which was inspired by migratory birds' behavior during their long-distance aerial migrations. The QANA is modeled by introducing long-term and short-term memories, a V-echelon communication topology, and quantum-based navigation with two mutation strategies and a qubit-crossover operator. To assign a mutation strategy to the flocks, we introduced the success-based population distribution (SPD) policy according to Definition 4, which uses the success rate of the mutation strategy in the previous iteration. Moreover, using the novel V-echelon communication topology can promote slow diffusion of unpromising information flow through the population by enhancing the population diversity and suspending premature convergence. The effectiveness and scalability of the proposed QANA were experimentally evaluated using benchmark functions, CEC 2018 with dimensions 30, 50, and 100 and CEC 2013 with dimension 1000. Besides, four engineering problems were considered to evaluate the applicability of the QANA to solve real-world problems. The superiority of the proposed algorithm was also statically analyzed using the Wilcoxon signed-rank sum, analysis of variance (ANOVA) and mean absolute error (MAE) tests. The experimental results show that the QANA is highly competitive with state-of-the-art SI and DE algorithms. The experiment and statistical results and the above-mentioned discussions support the following conclusions:

– The LTM and STM memories, defined in Definitions 1 and 2, allow adequate search space coverage in high-dimensional problems.
– Using the V-echelon communication topology influences the information flow between search agents, in which the spreading of reasonable solutions throughout the population is slowed down, discouraging stagnation and premature convergence.
– The quantum mutation strategy with two meaningful search strategies and a self-adaptive quantum orientation causes the search agents to converge to the global optimum faster than the compared algorithms.
– The qubit-crossover operator can maintain the population diversity of the QANA.

– The QANA can effectively explore the landscape using a multi-flock and qubit-crossover operator, enhancing diversity and landscape coverage.
– Performance index analysis in Fig. 13 shows the superiority of the proposed algorithm in terms of effectiveness over the contender algorithms.
– The results tabulated in Table 5 confirm that the proposed QANA is more scalable than other compared algorithms for solving large-scale global optimization (LSGO) problems.
– The experimental results and statistical analysis prove that the QANA is more efficient than the comparative algorithms for different unimodal, multimodal, hybrid, and composition problems.
– The QANA is applicable to solve real-world engineering optimization problems more precisely than the other compared algorithms.

To summarize the performance evaluation results, Table 13 presents the overall effectiveness (OE) of the QANA and contender algorithms based on their total performance shown in Tables 2–5. The OE of each algorithm was computed using Eq. (17), where the parameter N is the total number of tests, and L is the total number of losing tests for each algorithm.

$$OE = \left(\frac{N-L}{N}\right) \times 100 \tag{17}$$

Table13 Overall effectiveness of the QANA and contender algorithms.

Test functions	Unimodal/Multimodal/Hybrid/Composition					LSGO 2013	
Algorithms	30 (W|T|L)	50 (W|T|L)	100 (W|T|L)	Total (W|T|L)	OE (%)	1000 (W|T|L)	OE (%)
jDE	0|0|29	0|0|29	0|0|29	0|0|87	0%	0|0|15	0%
DE/BBO	0|2|27	1|1|27	3|2|24	4|5|78	10.35%	0|0|15	0%
CoDE	1|0|28	4|0|25	3|2|24	8|2|77	11.49%	3|0|12	20%
Jaya	0|0|29	0|0|29	0|0|29	0|0|87	0%	0|0|15	0%
MKE	2|0|27	2|1|26	1|0|28	5|1|81	6.90%	1|0|14	6.67%
SSA	0|2|27	0|1|28	1|0|28	1|3|83	4.60%	0|0|15	0%
EEGWO	0|0|29	0|0|29	0|0|29	0|0|87	0%	0|0|15	0%
WDE	0|0|29	0|0|29	0|0|29	0|0|87	0%	0|0|15	0%
MWOA	0|0|29	0|0|29	0|0|29	0|0|87	0%	0|0|15	0%
AOA	0|0|29	0|0|29	0|0|29	0|0|87	0%	0|0|15	0%
QANA	23|2|4	20|2|7	19|4|6	62|8|17	**80.46%**	11|0|4	**73.33%**

Considering the promising results of the QANA algorithm for solving single and continuous optimization problems in this work, further development of this algorithm for solving multi-objective and discrete real-world problems is suggested for future works. Moreover, we plan to apply the QANA algorithm to solve additional real-world optimization problems within the complex search space.

Acknowledgment

The authors would like to thank all anonymous reviewers for their valuable comments and suggestions on this paper.

Conflict of interest

The author declares that there is no conflict of interest regarding the publication of this article.

Appendix

Tension/compression spring problem: Three decision variables, wire diameter (d), mean coil diameter (D), and the number of active coils (N), were considered for formulating tension/compression spring problem, and Fig. A.1 shows the schematic of this problem. The weight of a tension/compression spring is the objective function that should be minimum, which is defined in Eq. (A.1).

$$
\begin{array}{ll}
\text{Consider} & \vec{x} = [x_1 x_2 x_3] = [d\ D\ N] \\
\text{Minimize} & f(\vec{x}) = (x_3 + 2)x_2 x_1^2 \\
\text{Subject to} & g_1(\vec{x}) = 1 - \frac{x_2^3 x_3}{71785 x_1^4} \leq 0, \\
& g_2(\vec{x}) = \frac{4x_2^2 - x_1 x_2}{12566(x_2 x_1^3 - x_1^4)} + \frac{1}{5108 x_1^2} - 1 \leq 0, \\
& g_3(\vec{x}) = 1 - \frac{140.45 x_1}{x_2^2 x_3} \leq 0, \\
& g_4(\vec{x}) = \frac{x_1 + x_2}{1.5} - 1 \leq 0. \\
\text{Variable range} & 0.05 \leq x_1 \leq 2.00, \\
& 0.25 \leq x_2 \leq 1.30, \\
& 2.00 \leq x_3 \leq 15.0
\end{array}
\tag{A.1}
$$

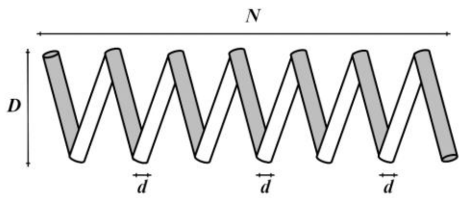

Fig. A. 1 Tension/compression spring problem

Pressure vessel design (PVD) problem: In this problem, the constraint decision variables include the thickness of the shell (T_s or x_1), thickness of the head (T_h or x_2), inner radius (R or x_3), and length of the cylindrical section of the vessel (L or x_4). The formula for this objective function is presented in Eq. (A.2). The schematic of the constraint PVD problem is illustrated in Fig. A.2.

$$
\begin{array}{ll}
\text{Consider} & \vec{x} = [x_1 x_2 x_3 x_4] = [T_s\ T_h\ R\ L], \\
\text{Minimize} & f(\vec{x}) = 0.6224 x_1 x_3 x_4 + 1.7781 x_2 x_3^2 + 3.1661 x_1^2 x_4 + 19.84\, x_1^2 x_3, \\
\text{Subject to} & g_1(\vec{x}) = -x_1 + 0.0193 x_3 \leq 0, \\
& g_2(\vec{x}) = -x_2 + 0.00954 x_3 \leq 0, \\
& g_3(\vec{x}) = -\pi x_3^2 x_4 - \frac{4}{3}\pi x_3^3 + 1{,}296{,}000 \leq 0, \\
& g_4(\vec{x}) = x_4 - 240 \leq 0,
\end{array}
\tag{A.2}
$$

Variable range	$0 \le x_1 \le 99$, $0 \le x_2 \le 99$, $10 \le x_3 \le 200$, $10 \le x_4 \le 200$

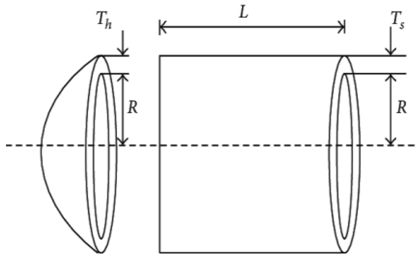

Fig. A. 2. Design of pressure vessel problem.

Three bar truss problem: This problem is defined in Eq. (A.3) with two constraint decision variables (x_1, x_2). The schematic of this problem is shown in Fig. A.3.

Consider $\vec{x} = [x_1 x_2] = [A_1\ A_2]$,

Min $f(\vec{x}) = \left(2\sqrt{2x_1} + x_2\right) \times l$,

Subject to

$$g_1(\vec{x}) = \frac{\sqrt{2}x_1 + x_2}{\sqrt{2}\,x_1^2 + 2x_1x_2} P - \sigma \le 0,$$
$$g_2(\vec{x}) = \frac{x_2}{\sqrt{2}x_1^2 + 2x_1x_2} P - \sigma \le 0, \quad (A.3)$$
$$g_3(\vec{x}) = \frac{1}{\sqrt{2}x_2 + x_1} P - \sigma \le 0,$$

Variable range $0 \le x_i \le 1, \quad i = 1,2$

$l = 100\text{cm}, P = 2\ \text{kN/cm}^2, \text{and}\ \ \sigma = 2\ \text{kN/cm}^2$

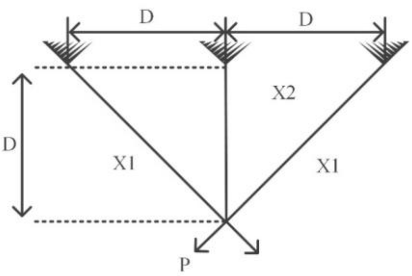

Fig. A. 3 Three bar truss problem

Welded beam problem: This problem is formulated using three constraint decision variables, i.e. the thickness of the weld (h or x_1), length of the clamped bar (l or x_2), height of the bar (t or x_3), and thickness of the bar (b or x_4), in Eq. (A.4). The fabrication cost of a welded beam is considered as an objective, and the schematic of this problem is presented in Fig. A.4.

Consider $\vec{x} = [x_1, x_2, x_3, x_4] = [h, l, t, b]$, (A.4)

Min $f(\vec{x}) = 1.10471x_1^2 x_2 + 0.04811x_3x_4(14.0 + x_2)$, Subject to

$$g_1(\vec{x}) = \tau(\vec{x}) - \tau_{max} \leq 0,$$
$$g_2(\vec{x}) = \sigma(\vec{x}) - \sigma_{max} \leq 0,$$
$$g_3(\vec{x}) = x_1 - x_4 \leq 0,$$
$$g_4(\vec{x}) = 1.10471x_1^2 + 0.04811x_3x_4(14.0 + x_2) - 5.0 \leq 0,$$
$$g_5(\vec{x}) = 0.125 - x_1 \leq 0,$$
$$g_6(\vec{x}) = \delta(\vec{x}) - \delta_{max} \leq 0,$$
$$g_7(\vec{x}) = P - P_c \leq 0,$$

Variable range $0.1 \leq x_i \leq 2, \quad i = 1,4, \qquad 0.1 \leq x_i \leq 10, \quad i = 2,3$

Where

$$\tau(\vec{x}) = \sqrt{(\tau')^2 + 2\tau'\tau''\frac{x_2}{2R} + (\tau'')^2},\ \tau' = \frac{P}{\sqrt{2}\,x_1x_2}, \tau'' = \frac{MR}{J}, M = P\left(L + \frac{x_2}{2}\right), R = \sqrt{\frac{x_2^2}{4} + (\frac{x_1+x_3}{2})^2}, \quad J = 2\left\{\sqrt{2}\,x_1x_2\left[\frac{x_2^2}{12} + \left(\frac{x_1+x_3}{2}\right)^2\right]\right\}, \sigma(\vec{x}) = \frac{6PL}{x_4x_3^2}, \delta(\vec{x}) = \frac{6PL^3}{E\,x_3^2\,x_4},$$

$$P_c(\vec{x}) = \frac{4.013E\sqrt{\frac{x_3^2x_4^6}{36}}}{E\,x_3^2\,x_4}\left(1 - \frac{x_3}{2L}\sqrt{\frac{E}{4G}}\right), P = 6000\ \text{lb}, L = 14\ \text{in.}, E = 30 \times 1^6\text{psi}, G = 12 \times 10^6\text{psi}, \tau_{max} = 13{,}600\ \text{psi}, \sigma_{max} = 30{,}000\ \text{psi}, \delta_{max} = 0.25\ \text{in.}$$

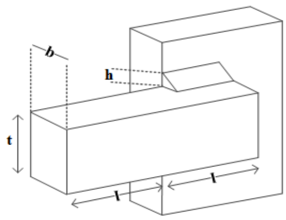

Fig. A. 4 Welded beam problem

References

Abdel-Basset, M., El-Shahat, D., Deb, K., Abouhawwash, M., 2020. Energy-aware whale optimization algorithm for real-time task scheduling in multiprocessor systems. Applied Soft Computing, 106349.

Abderazek, H., Yildiz, A.R., Sait, S.M., 2019. Mechanical engineering design optimisation using novel adaptive differential evolution algorithm. International Journal of Vehicle Design 80, 285-329.

Abualigah, L., Diabat, A., Mirjalili, S., Abd Elaziz, M., Gandomi, A.H., 2021. The arithmetic optimization algorithm. Computer methods in applied mechanics and engineering 376, 113609.

Ahandani, M.A., Alavi-Rad, H., 2012. Opposition-based learning in the shuffled differential evolution algorithm. Soft computing 16, 1303-1337.

Altabeeb, A.M., Mohsen, A.M., Ghallab, A., 2019. An improved hybrid firefly algorithm for capacitated vehicle routing problem. Applied Soft Computing 84, 105728.

Awad, N., Ali, M., Liang, J., Qu, B., Suganthan, P., 2016a. Problem definitions and evaluation criteria for the cec 2017 special sessionand competition on single objective real-parameter numerical optimization. Nanyang Technological University, Jordan University of Science and Technology and Zhengzhou University, Singapore and Zhenzhou, China, Tech. Rep 201611.

Awad, N.H., Ali, M.Z., Suganthan, P.N., Reynolds, R.G., 2016b. An ensemble sinusoidal parameter adaptation incorporated with L-SHADE for solving CEC2014 benchmark problems, 2016 IEEE congress on evolutionary computation (CEC). IEEE, pp. 2958-2965.

Awad, N.H., Ali, M.Z., Suganthan, P.N., Reynolds, R.G., 2017. CADE: a hybridization of cultural algorithm and differential evolution for numerical optimization. Information Sciences 378, 215-241.

Bajec, I.L., Heppner, F.H., 2009. Organized flight in birds. Animal Behaviour 78, 777-789.

Banaie-Dezfouli, M., Nadimi-Shahraki, M.H., Beheshti, Z., 2021. R-GWO: Representative-based grey wolf optimizer for solving engineering problems. Applied Soft Computing, 107328.

Beyer, H.-G., Schwefel, H.-P., 2002. Evolution strategies–A comprehensive introduction. Natural computing 1, 3-52.

Biswas, P.P., Suganthan, P.N., 2020. Large Initial Population and Neighborhood Search incorporated in LSHADE to solve CEC2020 Benchmark Problems, 2020 IEEE Congress on Evolutionary Computation (CEC). IEEE, pp. 1-7.

Brest, J., Greiner, S., Boskovic, B., Mernik, M., Zumer, V., 2006. Self-adapting control parameters in differential evolution: A comparative study on numerical benchmark problems. IEEE transactions on evolutionary computation 10, 646-657.

Brest, J., Maučec, M.S., 2008. Population size reduction for the differential evolution algorithm. Applied Intelligence 29, 228-247.
Brest, J., Maučec, M.S., Bošković, B., 2016. iL-SHADE: Improved L-SHADE algorithm for single objective real-parameter optimization, 2016 IEEE Congress on Evolutionary Computation (CEC). IEEE, pp. 1188-1195.
Brest, J., Maučec, M.S., Bošković, B., 2017. Single objective real-parameter optimization: Algorithm jSO, 2017 IEEE congress on evolutionary computation (CEC). IEEE, pp. 1311-1318.
Cai, Y., Wang, J., 2015. Differential evolution with hybrid linkage crossover. Information Sciences 320, 244-287.
Civicioglu, P., Besdok, E., Gunen, M.A., Atasever, U.H., 2020. Weighted differential evolution algorithm for numerical function optimization: a comparative study with cuckoo search, artificial bee colony, adaptive differential evolution, and backtracking search optimization algorithms. Neural Computing and Applications 32, 3923-3937.
Deb, K., Myburgh, C., 2017. A population-based fast algorithm for a billion-dimensional resource allocation problem with integer variables. European Journal of Operational Research 261, 460-474.
Deep, K., Thakur, M., 2007. A new mutation operator for real coded genetic algorithms. Applied mathematics and Computation 193, 211-230.
Deng, L.-B., Wang, S., Qiao, L.-Y., Zhang, B.-Q., 2017. DE-RCO: rotating crossover operator with multiangle searching strategy for adaptive differential evolution. IEEE Access 6, 2970-2983.
Dezfouli, M.B., Nadimi-Shahraki, M.H., Zamani, H., 2018. A Novel Tour Planning Model using Big Data, 2018 International Conference on Artificial Intelligence and Data Processing (IDAP). IEEE, pp. 1-6.
dos Santos Coelho, L., Ayala, H.V., Freire, R.Z., 2013. Population's variance-based adaptive differential evolution for real parameter optimization, 2013 IEEE congress on evolutionary computation. IEEE, pp. 1672-1677.
Eiben, A.E., Smith, J.E., 2015. Introduction to evolutionary computing. Springer.
Fan, H.-Y., Lampinen, J., 2003. A trigonometric mutation operation to differential evolution. Journal of global optimization 27, 105-129.
Gandomi, A.H., Alavi, A.H., 2012. Krill herd: a new bio-inspired optimization algorithm. Communications in nonlinear science and numerical simulation 17, 4831-4845.
Gandomi, A.H., Deb, K., Averill, R.C., Rahnamayan, S., Omidvar, M.N., 2019. Using semi-independent variables to enhance optimization search. Expert Systems with Applications 120, 279-297.
Ghosh, S., Roy, S., Das, S., Abraham, A., Islam, S.M., 2011. Peak-to-average power ratio reduction in OFDM systems using an adaptive differential evolution algorithm, 2011 IEEE Congress of Evolutionary Computation (CEC). IEEE, pp. 1941-1949.
Gong, W., Cai, Z., Ling, C.X., 2010. DE/BBO: a hybrid differential evolution with biogeography-based optimization for global numerical optimization. Soft Computing 15, 645-665.
Gupta, S., Deep, K., 2019. A novel random walk grey wolf optimizer. Swarm and evolutionary computation 44, 101-112.
Hatamlou, A., 2013. Black hole: A new heuristic optimization approach for data clustering. Information sciences 222, 175-184.
He, W., Bagherzadeh, S.A., Shahrajabian, H., Karimipour, A., Jadidi, H., Bach, Q.-V., 2020. Controlled elitist multi-objective genetic algorithm joined with neural network to study the effects of nano-clay percentage on cell size and polymer foams density of PVC/clay nanocomposites. Journal of Thermal Analysis and Calorimetry 139, 2801-2810.
Houssein, E.H., Mahdy, M.A., Eldin, M.G., Shebl, D., Mohamed, W.M., Abdel-Aty, M., 2021. Optimizing quantum cloning circuit parameters based on adaptive guided differential evolution algorithm. Journal of Advanced Research 29, 147-157.
Hussain, K., Salleh, M.N.M., Cheng, S., Shi, Y., 2019. On the exploration and exploitation in popular swarm-based metaheuristic algorithms. Neural Computing and Applications 31, 7665-7683.
Islam, S.M., Das, S., Ghosh, S., Roy, S., Suganthan, P.N., 2011. An adaptive differential evolution algorithm with novel mutation and crossover strategies for global numerical optimization. IEEE Transactions on Systems, Man, and Cybernetics, Part B (Cybernetics) 42, 482-500.
Karaboga, D., Basturk, B., 2007. A powerful and efficient algorithm for numerical function optimization: artificial bee colony (ABC) algorithm. Journal of global optimization 39, 459-471.
Karasu, S., Altan, A., Bekiros, S., Ahmad, W., 2020. A new forecasting model with wrapper-based feature selection approach using multi-objective optimization technique for chaotic crude oil time series. Energy 212, 118750.
Kaveh, A., Khayatazad, M., 2012. A new meta-heuristic method: ray optimization. Computers & structures 112, 283-294.
Khanum, R.A., Tairan, N., Jan, M.A., Mashwani, W.K., Salhi, A., 2016. Reflected adaptive differential evolution with two external archives for large-scale global optimization. International Journal of Advanced Computer Science and Applications 7, 675-683.
Kirkpatrick, S., Gelatt, C.D., Vecchi, M.P., 1983. Optimization by simulated annealing. science 220, 671-680.
Larrañaga, P., Lozano, J.A., 2001. Estimation of distribution algorithms: A new tool for evolutionary computation. Springer Science & Business Media.
LaTorre, A., Muelas, S., Peña, J.-M., 2013. Large scale global optimization: Experimental results with MOS-based hybrid algorithms, 2013 IEEE congress on evolutionary computation. IEEE, pp. 2742-2749.

LaTorre, A., Peña, J.-M., 2017. On the scalability of population restart mechanisms on large-scale global optimization, 2017 IEEE Congress on Evolutionary Computation (CEC). IEEE, pp. 1071-1078.
Li, X., Tang, K., Omidvar, M.N., Yang, Z., Qin, K., China, H., 2013. Benchmark functions for the CEC 2013 special session and competition on large-scale global optimization. gene 7, 8.
Long, W., Jiao, J., Liang, X., Tang, M., 2018. An exploration-enhanced grey wolf optimizer to solve high-dimensional numerical optimization. Engineering Applications of Artificial Intelligence 68, 63-80.
Lu, H., Liu, Y., Cheng, S., Shi, Y., 2020. Adaptive online data-driven closed-loop parameter control strategy for swarm intelligence algorithm. Information Sciences.
Maeda, K., Henbest, K.B., Cintolesi, F., Kuprov, I., Rodgers, C.T., Liddell, P.A., Gust, D., Timmel, C.R., Hore, P.J., 2008. Chemical compass model of avian magnetoreception. Nature 453, 387-390.
Mafarja, M., Aljarah, I., Faris, H., Hammouri, A.I., Ala'M, A.-Z., Mirjalili, S., 2019. Binary grasshopper optimisation algorithm approaches for feature selection problems. Expert Systems with Applications 117, 267-286.
Mallipeddi, R., Suganthan, P.N., 2010. Differential evolution algorithm with ensemble of parameters and mutation and crossover strategies, International conference on swarm, evolutionary, and memetic computing. Springer, pp. 71-78.
Mallipeddi, R., Suganthan, P.N., Pan, Q.-K., Tasgetiren, M.F., 2011. Differential evolution algorithm with ensemble of parameters and mutation strategies. Applied soft computing 11, 1679-1696.
Maučec, M.S., Brest, J., 2019. A review of the recent use of Differential Evolution for Large-Scale Global Optimization: An analysis of selected algorithms on the CEC 2013 LSGO benchmark suite. Swarm and Evolutionary Computation 50, 100428.
Meng, Z., Pan, J.-S., 2016. Monkey king evolution: a new memetic evolutionary algorithm and its application in vehicle fuel consumption optimization. Knowledge-Based Systems 97, 144-157.
Meng, Z., Pan, J.-S., 2018. QUasi-Affine TRansformation Evolution with External ARchive (QUATRE-EAR): an enhanced structure for differential evolution. Knowledge-Based Systems 155, 35-53.
Meng, Z., Pan, J.-S., 2019. HARD-DE: Hierarchical archive based mutation strategy with depth information of evolution for the enhancement of differential evolution on numerical optimization. IEEE Access 7, 12832-12854.
Meng, Z., Pan, J.-S., Kong, L., 2018. Parameters with adaptive learning mechanism (PALM) for the enhancement of differential evolution. Knowledge-Based Systems 141, 92-112.
Mirjalili, S., Gandomi, A.H., Mirjalili, S.Z., Saremi, S., Faris, H., Mirjalili, S.M., 2017. Salp Swarm Algorithm: A bio-inspired optimizer for engineering design problems. Advances in Engineering Software 114, 163-191.
Mirjalili, S., Lewis, A., 2016. The whale optimization algorithm. Advances in engineering software 95, 51-67.
Mirjalili, S., Mirjalili, S.M., Lewis, A., 2014. Grey wolf optimizer. Advances in engineering software 69, 46-61.
Mouritsen, H., 2018. Long-distance navigation and magnetoreception in migratory animals. Nature 558, 50-59.
Nadimi-Shahraki, M.H., Taghian, S., Mirjalili, S., 2020a. An Improved Grey Wolf Optimizer for Solving Engineering Problems. Expert Systems with Applications, 113917.
Nadimi-Shahraki, M.H., Taghian, S., Mirjalili, S., Faris, H., 2020b. MTDE: An effective multi-trial vector-based differential evolution algorithm and its applications for engineering design problems. Applied Soft Computing, 106761.
Nielsen, M.A., Chuang, I.L., 2001. Quantum computation and quantum information. Phys. Today 54, 60.
Olorunda, O., Engelbrecht, A.P., 2008. Measuring exploration/exploitation in particle swarms using swarm diversity, 2008 IEEE congress on evolutionary computation (IEEE world congress on computational intelligence). IEEE, pp. 1128-1134.
Pashaei, E., Aydin, N., 2017. Binary black hole algorithm for feature selection and classification on biological data. Applied Soft Computing 56, 94-106.
Price, K., Storn, R.M., Lampinen, J.A., 2006. Differential evolution: a practical approach to global optimization. Springer Science & Business Media.
Qin, A.K., Huang, V.L., Suganthan, P.N., 2008. Differential evolution algorithm with strategy adaptation for global numerical optimization. IEEE transactions on Evolutionary Computation 13, 398-417.
Qin, A.K., Suganthan, P.N., 2005. Self-adaptive differential evolution algorithm for numerical optimization, 2005 IEEE congress on evolutionary computation. IEEE, pp. 1785-1791.
Rahnamayan, S., Tizhoosh, H.R., Salama, M.M., 2008. Opposition-based differential evolution. IEEE Transactions on Evolutionary computation 12, 64-79.
Rao, R., 2016. Jaya: A simple and new optimization algorithm for solving constrained and unconstrained optimization problems. International Journal of Industrial Engineering Computations 7, 19-34.
Salehinejad, H., Rahnamayan, S., 2016. Effects of centralized population initialization in differential evolution, 2016 IEEE Symposium Series on Computational Intelligence (SSCI). IEEE, pp. 1-8.
Sayarshad, H.R., 2010. Using bees algorithm for material handling equipment planning in manufacturing systems. The International Journal of Advanced Manufacturing Technology 48, 1009-1018.
Simon, D., 2008. Biogeography-based optimization. IEEE transactions on evolutionary computation 12, 702-713.
Soleimanpour-Moghadam, M., Nezamabadi-Pour, H., Farsangi, M.M., 2014. A quantum inspired gravitational search algorithm for numerical function optimization. Information Sciences 267, 83-100.

Srikanth, K., Panwar, L.K., Panigrahi, B.K., Herrera-Viedma, E., Sangaiah, A.K., Wang, G.-G., 2018. Meta-heuristic framework: quantum inspired binary grey wolf optimizer for unit commitment problem. Computers & Electrical Engineering 70, 243-260.
Storn, R., Price, K., 1995. Differential evolution–a simple and efficient adaptive scheme for global optimization over continuous spaces: technical report TR-95-012. International Computer Science, Berkeley, California.
Storn, R., Price, K., 1997. Differential evolution–a simple and efficient heuristic for global optimization over continuous spaces. Journal of global optimization 11, 341-359.
Sun, Y., Wang, X., Chen, Y., Liu, Z., 2018. A modified whale optimization algorithm for large-scale global optimization problems. Expert Systems with Applications 114, 563-577.
Taghian, S., Nadimi-Shahraki, M.H., 2019a. A Binary Metaheuristic Algorithm for Wrapper Feature Selection. International Journal of Computer Science Engineering (IJCSE) 8, 168-172.
Taghian, S., Nadimi-Shahraki, M.H., 2019b. Binary Sine Cosine Algorithms for Feature Selection from Medical Data. arXiv preprint arXiv:1911.07805.
Taghian, S., Nadimi-Shahraki, M.H., Zamani, H., 2018. Comparative analysis of transfer function-based binary Metaheuristic algorithms for feature selection, 2018 International Conference on Artificial Intelligence and Data Processing (IDAP). IEEE, pp. 1-6.
Talbi, E.-G., 2009. Metaheuristics: from design to implementation. John Wiley & Sons.
Tanabe, R., Fukunaga, A., 2013. Success-history based parameter adaptation for differential evolution, 2013 IEEE congress on evolutionary computation. IEEE, pp. 71-78.
Tanabe, R., Fukunaga, A.S., 2014. Improving the search performance of SHADE using linear population size reduction, 2014 IEEE congress on evolutionary computation (CEC). IEEE, pp. 1658-1665.
Tayarani-N, M.-H., Akbarzadeh-T, M.-R., 2014. Magnetic-inspired optimization algorithms: Operators and structures. Swarm and Evolutionary Computation 19, 82-101.
Tong, L., Dong, M., Jing, C., 2018. An improved multi-population ensemble differential evolution. Neurocomputing 290, 130-147.
Vieira, S.M., Mendonça, L.F., Farinha, G.J., Sousa, J.M., 2013. Modified binary PSO for feature selection using SVM applied to mortality prediction of septic patients. Applied Soft Computing 13, 3494-3504.
Wang, K., Mattern, E., Ritz, T., 2006. On the use of magnets to disrupt the physiological compass of birds. Physical Biology 3, 220.
Wang, S., Li, Y., Yang, H., Liu, H., 2018. Self-adaptive differential evolution algorithm with improved mutation strategy. Soft Computing 22, 3433-3447.
Wang, X., Zhao, S., Jin, Y., Zhang, L., 2013. Differential evolution algorithm based on self-adaptive adjustment mechanism, 2013 25th Chinese Control and Decision Conference (CCDC). IEEE, pp. 577-581.
Wang, Y., Cai, Z., Zhang, Q., 2011. Differential evolution with composite trial vector generation strategies and control parameters. IEEE transactions on evolutionary computation 15, 55-66.
Wang, Y., Cai, Z., Zhang, Q., 2012. Enhancing the search ability of differential evolution through orthogonal crossover. Information Sciences 185, 153-177.
Wang, Y., Li, H.-X., Huang, T., Li, L., 2014. Differential evolution based on covariance matrix learning and bimodal distribution parameter setting. Applied Soft Computing 18, 232-247.
Wilcoxon, F., 1992. Individual comparisons by ranking methods, Breakthroughs in statistics. Springer, pp. 196-202.
Wiltschko, R., Wiltschko, W., 2009. Avian navigation. The Auk 126, 717-743.
Wu, G., Mallipeddi, R., Suganthan, P.N., Wang, R., Chen, H., 2016. Differential evolution with multi-population based ensemble of mutation strategies. Information Sciences 329, 329-345.
Wu, G., Shen, X., Li, H., Chen, H., Lin, A., Suganthan, P.N., 2018. Ensemble of differential evolution variants. Information Sciences 423, 172-186.
Wu, H., Bagherzadeh, S.A., D'Orazio, A., Habibollahi, N., Karimipour, A., Goodarzi, M., Bach, Q.-V., 2019. Present a new multi objective optimization statistical Pareto frontier method composed of artificial neural network and multi objective genetic algorithm to improve the pipe flow hydrodynamic and thermal properties such as pressure drop and heat transfer coefficient for non-Newtonian binary fluids. Physica A: Statistical Mechanics and its Applications 535, 122409.
Yang, Q., Xie, H.-Y., Chen, W.-N., Zhang, J., 2016. Multiple parents guided differential evolution for large scale optimization, 2016 IEEE Congress on Evolutionary Computation (CEC). IEEE, pp. 3549-3556.
Yang, X.S., Gandomi, A.H., 2012. Bat algorithm: a novel approach for global engineering optimization. Engineering computations.
Yang, Z., Tang, K., Yao, X., 2008. Self-adaptive differential evolution with neighborhood search, 2008 IEEE Congress on Evolutionary Computation (IEEE World Congress on Computational Intelligence). IEEE, pp. 1110-1116.
Zahrani, H.K., Nadimi-Shahraki, M.H., Sayarshad, H.R., 2021. An intelligent social-based method for rail-car fleet sizing problem. Journal of Rail Transport Planning & Management 17, 100231.
Zamani, H., Nadimi-Shahraki, M.H., 2016. Feature selection based on whale optimization algorithm for diseases diagnosis. International Journal of Computer Science and Information Security 14, 1243.
Zamani, H., Nadimi-Shahraki, M.H., Gandomi, A.H., 2019. CCSA: Conscious Neighborhood-based Crow Search Algorithm for Solving Global Optimization Problems. Applied Soft Computing 85, 105583.
Zhang, J., Sanderson, A.C., 2009. JADE: adaptive differential evolution with optional external archive. IEEE Transactions on evolutionary computation 13, 945-958.

Zhang, X., Wu, C., Li, J., Wang, X., Yang, Z., Lee, J.-M., Jung, K.-H., 2016. Binary artificial algae algorithm for multidimensional knapsack problems. Applied Soft Computing 43, 583-595.
Zhang, Y., Berman, G.P., Kais, S., 2015. The radical pair mechanism and the avian chemical compass: Quantum coherence and entanglement. International Journal of Quantum Chemistry 115, 1327-1341.
Zhong, J., Cai, W., 2015. Differential evolution with sensitivity analysis and the Powell's method for crowd model calibration. Journal of computational science 9, 26-32.